TWO-DIMENSIONAL STRUCTURAL VIBRATION INDUCED BY FLUID FLOW PAST A CIRCULAR CYLINDRICAL BODY

by

YU-MIN CHOW
B.S., National Taiwan University
Taipei, Taiwan, Republic of China. 1954

A THESIS SUBMITTED IN PARTIAL FULFILMENT OF
THE REQUIREMENTS FOR THE DEGREE OF

Master of Applied Science

in the Department

of

CIVIL ENGINEERING

We accept this thesis as conforming
to the required standard

THE UNIVERSITY OF BRITISH COLUMBIA

April, 1964

In presenting this thesis in partial fulfilment of the requirements for an advanced degree at the University of British Columbia, I agree that the Library shall make it freely available for reference and study. I further agree that permission for extensive copying of this thesis for scholarly purposes may be granted by the Head of my Department or by his representatives. It is understood that copying or publication of this thesis for financial gain shall not be allowed without my written permission.

Yu-min Chow

Department of Civil Engineering

The University of British Columbia,
Vancouver 8, Canada

Date May 1, 1964

Abstract

The investigation is concerned with the vibrational response of a circular cylindrical body when subjected to oscillating lift and drag forces of varying frequency. The cylindrical body was mounted on a long flexible cantilever and the stiffness of the cantilever could be varied to study the effects of resonance, amplitude and induced damping. An explanation of the two-dimensional excitation due to vortex shedding is presented.

Both longitudinal and transverse vibrations were induced and the frequency of the excitation in the longitudinal direction was about twice that in the lateral. Therefore, for equal structural natural frequencies in the lateral and longitudinal directions, resonance in the lateral direction will occur at twice the velocity of the longitudinal resonance, assuming the Strouhal Number to be constant in this range. Coefficients of the elastic response forces, in both longitudinal and lateral directions near the lonitudinal resonance, were plotted for comparison.

The development of irregularity in the lateral vibrating oscillogram caused by the longitudinal vibration was demonstrated. In the critical Reynolds Number range the effect of a fixed eddy-starter wire was investigated and the excitations in both lateral and longitudinal directions were altered.

The resonance of longitudinal vibration occurs at $^{V}/V_{res}$ = 0.3 to 0.5. Lateral amplitude in this region is also increased. The peak of the curve: S_y vs R_e, in the region of longitudinal resonance, approaches tengentially the curve: S_x vs R_e. The structural response coefficient of vibrating lift and drag rises at longitudinal resonance to a value of 3.0 to 8.0, but drops quickly after resonance. The damping coefficients of the structure are in the range of 0.25 to 0.60.

Since the motion of the vibration may influence the oscillating lift and drag due to the eddy shedding, this study presents an investigation of the longitudinal and lateral resonances in a range of R_e: $5 \times 10^3 - 3 \times 10^5$, and the interaction of the excitation between the oscillating lift and drag with the two-dimensional elastic response forces.

ACKNOWLEDGEMENT

The author wishes to express his gratitude to Dr. M.C. Quick for his guidance and criticism in the experimental work and the writing of the thesis. The author is also grateful to Prof. J.F. Muir, head of Civil Engineering Department, for his comments and the grant of the assistantship.

The experimental work was carried out in the hydraulic laboratory, Dept. of Civil Engineering, and appreciation is also expressed by the author to the staffs in the workshop.

TABLE OF CONTENTS

Tables

Figures

Two-Dimensional Structural Vibration Induced By Fluid Flow Past A Circular Cylindrical Body

I. Introduction:

Violent vibrations of various types of structures submerged in moving water are sometimes observed even in flows of moderately low velocity. Slender tall bodies such as a stack, an antenna or a sounding-rod, which are subject to fluid flow, may vibrate in response to longitudinal as well as lateral vibrating forces. The eddy shedding from unstable shear layers near the separation points behind a body in a moving fluid or a body moving in a fluid will give rise to an oscillating pressure distribution on the boundary of the body in the separation zone, the resultant alternating force in its vector sense will give a two-dimensional excitation to the moving body. In a vibrating system with two-dimensional freedom, the vector sum of alternating forces can give rise to longitudinal and lateral as well as torsional resultants causing vibration. This makes the vibration condition very complicated even in the region where the velocity is far below the lateral resonant velocity. Therefore the subject of this investigation is the relationship of lateral and longitudinal vibration characteristics, and their interactions.

The starting point of the shear layer intersects the boundary of the body, which stays in the flowing fluid, at separation point. The location of the separation point varies with the circulation of the shedding vortex, hence the mechanics in the shear layer may change accordingly. Oscillation of the solid boundary in either the longitudinal or lateral direction causes the shear layer to take on a wave pattern and also increases its instability. Therefore, additional distortion of the eddy shedding vortex alters the excitation, resulting in an irregular vibrating path. In order to obtain evidence to explain this irregularity, oscillograms were recorded by pen recorders in both the longitudinal and lateral direction separately and simultaneously.

There are three types of excitation in vibration: forced, self-excited and controlled. Self-excited vibration always occurs at its natural frequency, while forced vibration follows the frequency of the alternating external force. At resonance the frequencies of forced and self-excited vibrations coincide, and large amplification of response occurs and is only limited by the induced damping. If the vibration of the body influences the oscillating flow pattern, the resulting vibration is no longer either self-excited or forced, and belongs to the category of controlled vibration (1).[1]

The investigation of the oscillating fluid pressure around the cylinder has been done by several investigations, such as D.M. McGregor (5) and J.H. Gerrard (10). The measurements, obtained either from the study of stationary cylinders or from cylinders held rigidly enough to produce forced vibration under small vibrating amplitude, represent the oscillating fluid force in various flow conditions. This gives design data, presuming the structure to be stiff enough to prevent itself from vibrating under the fluid forces. The lift coefficient (5) is about 0.6 while the drag coefficient is approximately 0.06, both refer to oscillating parts.

Sometimes the structure is allowed to move or is flexible in nature, such as hydraulic gates or suspension bridges respectively. The motion of the structural vibration influences the fluid force, and vice versa. Therefore this study investigates the structural response forces during finite

1 Numbers in brackets refer to the bibliography.

amplitude motion excited by the fluid force. All the test runs allow the structure to have finite amplitude during vibration. A structure of two-dimensional freedom with equal natural frequencies in lateral and longitudinal direction was used. The irregular oscillograms of controlled vibration are recorded and analysed for Reynolds Numbers varying from 5×10^3 to 3×10^5, (for velocity ratio: $\frac{V}{V_{res}} = 0.2$ to 0.9). The longitudinal vibration appeared at a velocity ratio as low as 0.4 which is considerably lower than that of lateral resonance. In the present investigation the maximum velocity ratio attainable was limited by the maximum rate of flow of water available, combined with limitations on depth and velocity set by critical flow conditions.

II. Basic concepts

Introduction The wake behind a moving body in a real fluid represents a discontinuous flow phenomenon which is bounded by the thin shear layer known as a vortex sheet. The pattern of a double row of vortices originating from opposite sides of the body changes with growing R_e. In the range of R_e used in these experiments, say 5×10^3 to 3×10^5 the oscillating force appears to be due to eddy shedding.

In considering the vibration of a body in a moving fluid there are three major aspects to be considered. Firstly these are the fluid pressures and shears transmitted to the surface of the body, which give rise to a net oscillating force acting on the structure. Secondly there is the vibrational characteristics of the structure which may have several modes of vibration. Thirdly there is the modification of the flow pattern by the structural vibration and the possibility of self excitation. The first two aspects will now be considered independently and then some attempts will be made to discuss the third complex aspect of interaction.

<u>Blasius theorem</u> From Blasius theorem the resultant fluid force x, y in an ideal uniform flow with circulation can be expressed (4) by:

$$X - iY = \frac{i}{2} \rho \oint \left(\frac{dw}{dz}\right)^2 dz$$

where: $w = U\left(z + \frac{a^2}{z}\right) + \frac{i\Gamma}{2\pi} \text{In } z$

Using the Cauchy integral theorem and its extension, and with $\frac{dw}{dz}$ resulting from flow around cylinder with circulation, it is found that:

$X = 0$ i.e. Drag is zero

$Y = \rho \Gamma U$ i.e. lift depends on U and Γ.

This gives the force acting on the cylinder for ideal flow without separation but with circulation. For two-dimensional vibration, the oscillating pressure due to periodic change of circulation is an essential factor.

<u>Oscillating pressure study</u>: An oscillating pressure study by D.M. McGrefor(5) included a series of experimental and some mathematical steps. The local pressure is obtained from the Bernoulli equation:

$$\Delta p = \frac{\rho}{2}\left(U^2 - v^2\right) - \rho \frac{\partial \phi}{\partial t}$$

In the complex potential, in order to maintain the cylinder surface as a streamline, two vortices of equal strength but opposite sign were located at distances a and $\frac{a^2}{b}$ away (Fig. 1a) from the origin; so that one lies outside and one inside the cylinder:

$$\omega = U\left(z + \frac{a^2}{z}\right) + \frac{i\Gamma}{2\pi} \text{In } \frac{z - b}{z - a^2/b}$$

Assuming a periodic circulation of $\Gamma_m \text{ Sin } \omega t$ due to opposite eddy shedding, the pressure coefficient will be:

$$C_p = \frac{\Gamma_m}{Ua} f\left(\psi, \psi_1, \psi_2\right)$$

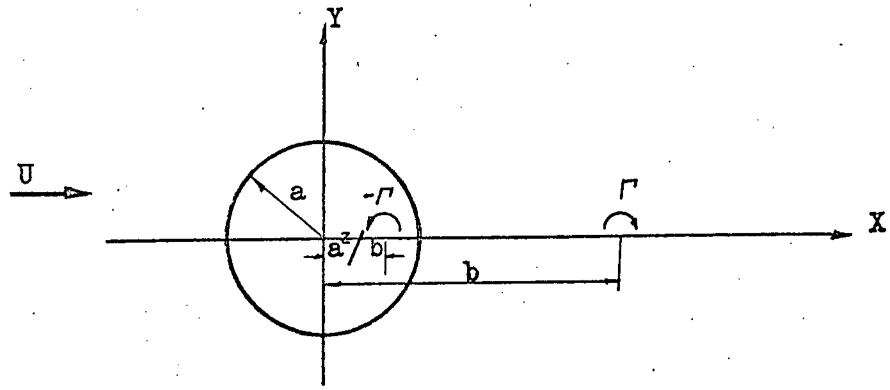

Fig. 1a

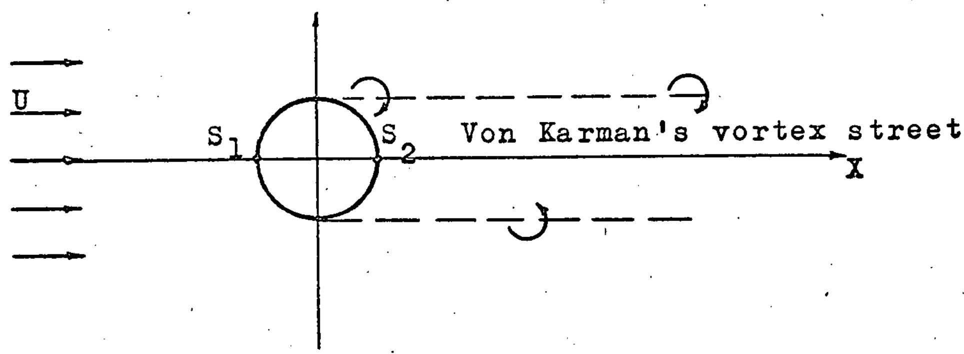

Fig. 1b

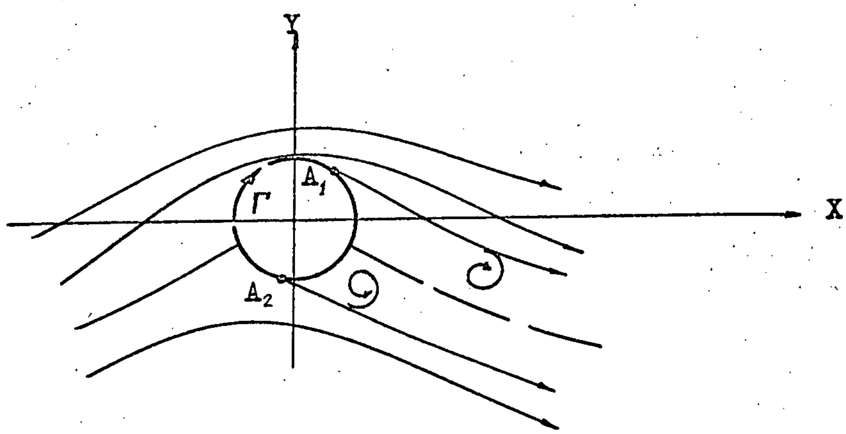

Fig. 1c

Fig. 1 Circular cylinder in uniform flow with Von Karman's vortex street where ψ, ψ_1, ψ_2 are the arguments in polar ordinates. Since, at any instant the flow in front of the point of separation can be treated as ideal and that in the wake as being altered, this reveals only some aspects of local pressure variation due to the shedding of vortices.

The oscillating pressure change around the various positions on the cylinder measured by McGregor, in a plotted relation between frequency and pressure coefficient in a given flow, appeared in two peaks which were called the fundamental and secondary harmonic frequencies. The fundamental frequency peak, about 165 cps, occured at 90^o position from the upstream stagnation point of the cylinder, while the secondary harmonic frequency, about 330 cps, appeared at 180^o. Therefore, if the two-dimensional vibration is excited by these oscillating pressures, the frequency of longitudinal vibration will be twice that in the lateral direction.

This study is very interesting and its results are supported by the finding of the present experiments.

<u>Response of elastic supported structure to eddy shedding force</u>

If a structure is acted upon by externally applied oscillating fluid force, a time-dependent motion* will be set up. The forced vibration can be expressed (6) by:

$$M\ddot{y} + D(t) + kY = F(t)$$

where: $F(t) = F_K = q\ A\ c_K \sin 2\pi ft$

q = stagnation pressure

$D(t)$ = damping function

A = area of body projected on fluid stream

F_K = Von Karmann vortex shedding force

f = frequency of eddy shedding

---

* Appendix I

The amplitude ratio of a system with a single degree of freedom and having viscous damping, may be written:

$$\frac{Y}{d} = \frac{c_1\ c_K\ \Omega^2/k}{\sqrt{(1+\Omega^2)^2 + (\frac{\beta}{\pi}\Omega^2)}}$$

where: c_1 is constant for a given system

c_K : coefficient.

Ω : ratio of the frequency of forcing function to natural frequency.

β : damping decrement.

Since there is no complete hydrodynamic theory for separated flow, the response function of an elastic system could be treated by quasi-steady theory.*

An estimate of the natural frequency of the system may be made by deflecting it and allowing it to vibrate freely. The resulting damping curve can also be used to calculate the value β. The damping will change with the velocity of flow and with amplitude of vibration. It should also be remembered that the eddy shedding frequency and the width of the vortex street will be altered by the amplitude of vibration.

III. Qualitative explanation of the two-dimensional vibration phenomenon:

Shear layer In the ideal flow, a uniform flow and a doublet gives the symmetrical flow pattern with two stagnation points S_1 and S_2 (Fig. 1b). From the boundary layer theory and the energy theorem, an expression:

$$\left(\frac{\partial^2 u}{\partial y^2}\right)_{y=0} = \frac{1}{\mu}\ \frac{dp}{dx}$$

can be obtained which reveals that the separation phenomenon will take place on the rear surface of the cylinder, which is a region of rising pressure

* Appendix II

and potential flow reversal in the boundary layer.

Two separation points A_1 and A_2 are indicated (Fig. 1c). Due to the reversal of flow, a thin shear layer is formed with a rolling eddy train along its path starting from the separation point and decaying in the downstream direction.

Lateral vibrating velocity According to the Kelvin's circulation theorem there is zero net vorticity and therefore every time a vortex is shed there is a circulation around the cylinder with opposite sign to that of the shedding vortex. This circulation with uniform flow generates a lift force and moves the separation points back and forth (Fig. 1c). When the circulation changes: $\Gamma \rightarrow o \rightarrow -\Gamma$, the separation points move to positions opposite to the previous ones, as in Fig. 1c. Hence the wake shifts repeatedly from left to right.

An elastic supported body acted on by this periodic force will vibrate in a direction perpendicular to the direction of the uniform flow. If the eddy shedding frequency is lower or equal to the natural frequency of the structural vibration, the sinusoidal lateral velocity of vibration can be expressed:

$$V_y = V_{ym} \operatorname{Sin} \omega t$$

where: V_{ym} = instantaneous maximum lateral vibrating velocity.

When the eddy shedding frequency is higher than the natural frequency of the elastic system, the pulsating force will run out of phase with the response of structure. Then the amplitude will diminish quickly to a very small value. A vibration in random nature will be resulted.

Longitudinal oscillating force X

i. With no lateral vibration: When a vortex is shedding, growing and passing downstream (Fig. 1c) the tangential velocity at the circumference of rear part of the cylinder changes according to the velocity distribution of the vortex. One eddy will give one complete cycle of the velocity variation. In the meantime, from energy theorem the oscillating pressure in longitudinal direction also completes one periodic excitation to the vibration of the structure. Therefore, the oscillating drag has a frequency twice that of pulsating lift.

ii. Reinforced by lateral vibration: When the vortices are shedding alternatively from the cylinder, the circulation around the cylinder also changes in value from positive to negative. Therefore an assumption is made:

$$\Gamma = \Gamma_m \operatorname{Sin} \omega t$$

Considering the cylinder travelling from A to B (Fig. 2a), the sum of the velocity vectors is:

$$V = (U^2 + V_y^2)^{1/2}$$

toward the cylinder with an attack angle α. From the Magnus effect, a lift force L exists, which gives two components in x and y-direction: X, Y:

$$X = \rho U (\Gamma_m \operatorname{Sin} \omega t) \operatorname{Sin} \alpha$$

$$Y = \rho U (\Gamma_m \operatorname{Sin} \omega t) \operatorname{Cos} \alpha$$

From the above equation, the longitudinal force in two-dimensional vibration is a function of lift and attack angle. When the cylinder, after reaching point c, vibrates back to D (Fig. 2b), the Y-component of the lift changes its direction, but the X-component still acts in a positive x-direction. From that the angle of attack is zero, and assuming the circulation to be zero at points A, C and E, components X and Y will be

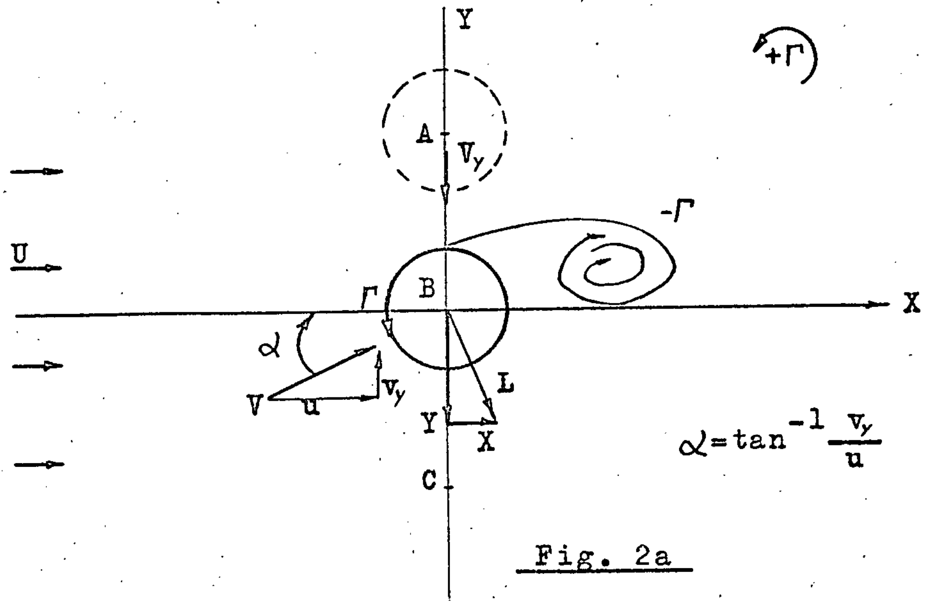

Fig. 2a

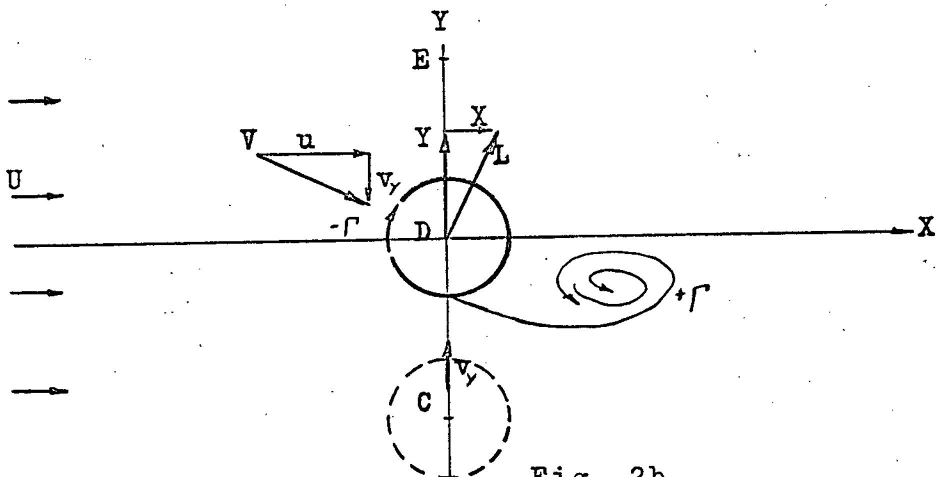

Fig. 2b

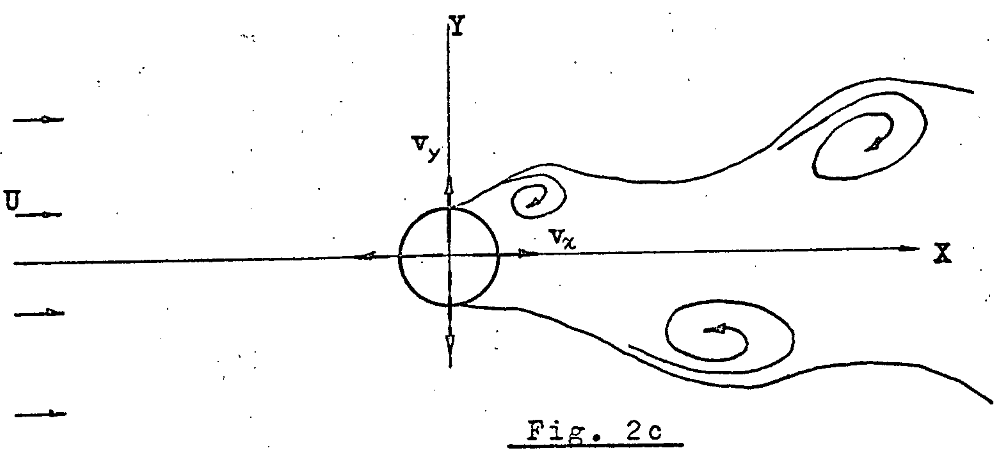

Fig. 2c

Fig. 2 Theoretical oscillating lift and drag zero at these locations. This means that when the variation of lift force completes one cycle, the longitudinal force will complete two cycles in the same time. Therefore, the frequency of excitation in the longitudinal direction will be twice that in the lateral. This relation is indicated in Fig. 3.

So far it has been assumed that vortex shedding is two dimensional and is therefore in phase along the axis of the cylinder. In a real fluid this may not be true and the phase of eddy shedding may change along the axis of the cylinder. Any distorsion (8) of the vortex along its axis or other small disturbance will change the value of the excitation, the response of the elastic structure will then change accordingly. It is considered, although there is at present no evidence to support it, that once a vibration commences, all the vortex shedding along the cylinder will be forced into phase.

Resultant vibration of two-dimensional periodic phenomena

In the two-dimensional vibration, the longitudinal velocity of cylinder will also vary with time (Fig. 4); this means that an additional periodic variation of V_x will be superposed on the uniform velocity U. Since the lift force is a function of longitudinal velocity, the resulting lift forces and displacements will present themselves as a resultant of two-dimensional periodic combinations.

Therefore it can be seen that a longitudinal vibration will tend to excite additional lateral vibrational forces, and conversely a lateral vibration will cause additional longitudinal vibrational forces. This complex interaction is demonstrated by some of tests in which self-excited vibrations appear. It has not been found possible to discuss the interaction quantitatively but a qualitative understanding is possible. The fact that the two modes differ in frequency by a factor of two is all important, because it presents a double resonance at the fundamental. It is intersting to consider

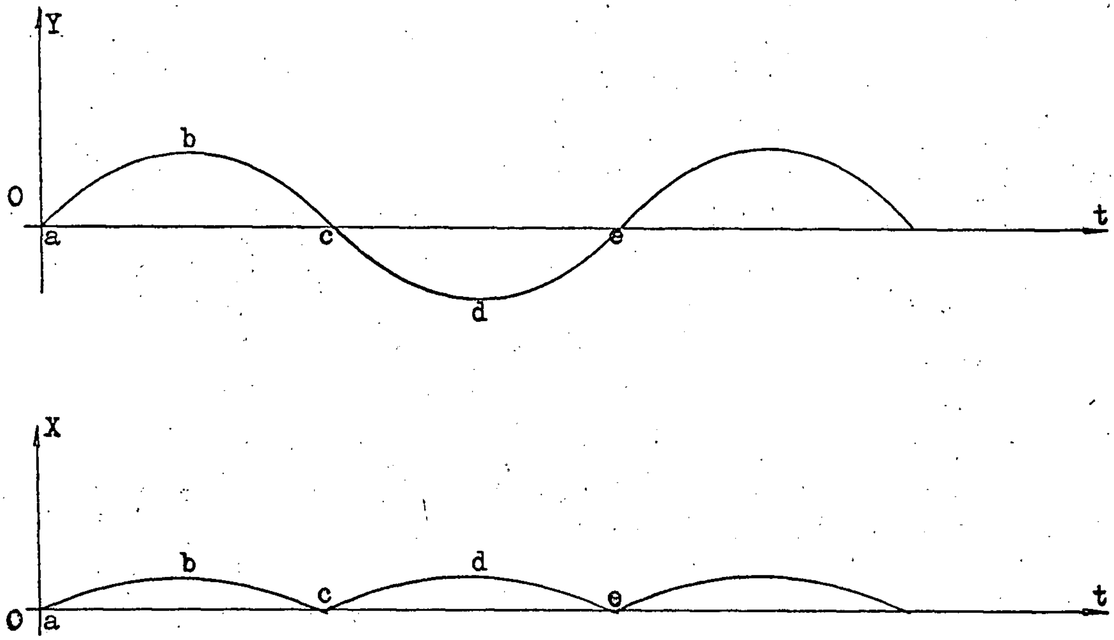

Fig. 3 Frequency of ideal oscillating lift and drag

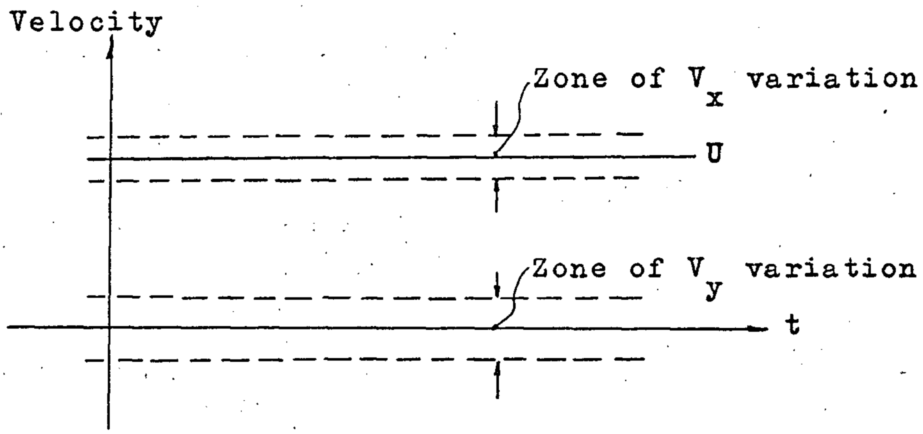

Fig. 4 Sinusoidal variation of V_x and V_y

what might happen if the lateral vibration were in the second mode whilst the longitudinal vibration coincided with the first mode, assuming the first and second modes to have a frequency ratio of two.

Stability of two-dimensional vibration

Since the frequency of excitation in longitudinal direction is twice that of the lateral, the velocity of resonance in the longitudinal direction will be half that of the lateral, if natural frequencies are the same in both directions. In a situation of self excitation the stability of the system must be considered. If the induced excitation increases more rapidly than the damping force, violent two-dimensional vibration results, hence the structure will be overloaded.

Conclusion

Stationary cylinder: Starting from Von-Karman's theoretical vortex street with a stationary cylinder, due to the circulation caused by shedding vortex, the vortex street may shift left and right resulting a wave-like wake path. This will produce a smaller component of oscillating drag, as vortices of alternate sign grow and pass downstream. It has twice the frequency of the oscillating lift and arises from a changing pressure distribution excitation in the longitudinal direction.

Vibrating cylinder: Since the lateral vibration gives a periodic V_y variation, a periodic x-component arises with a frequency twice that of the lateral. This strengthened oscillating drag will cause a strong excitation if its frequency is near the natural frequency of the structure.

IV. Apparatus and Instrumentation

4.1 General consideration:

Since this experiment emphasized two-dimensional vibration as well as the relationship of its frequency, phase and amplitude, a constant flexural system with low natural frequency and recordable lift and drag force was required. The 30" wide water flume and steel cantilever mounting were chosen.

A hollow brass cylinder 2" in diameter was first used as a test body. At both ends, 6" diameter discs were provided as split walls to prevent secondary vorticity. A 3/4" square steel bar served as a flexural structure mounted on a 5" I-beam which, supported on concrete walls, was strong enough to hold the vibrating test body.

From the relation: $S = \frac{fD}{V}$ for stationary cylinder of 2" diameter, if the velocity of flow is in the range of 0.50 fps to 4.35 fps, the frequency of eddy shedding will be about 0.6 cps to 5.3 cps respectively. If a flexural cantilever with a frequency about 5 cps in both longitudinal and lateral direction is chosen, it will give longitudinal as well as lateral resonance in the flow range. In order to make the strain in strain gauge recordable, strain was limited in the range of: 50 to 2000 micro-in/in.

The natural frequency was checked approximately by the equation:

$$f = c\sqrt{\frac{EI}{ML^4}}$$ where: c: coe. including damping effect.

Four combinations, with steel and aluminum material, 2" and 4" circular cylinder, were selected and listed in Table VII. Four strain gauges located at the upper end of the cantilever gave the vibrating response forces in two directions, and below the resonance condition these response forces gave the frequency and amplitude of the vibration.

4.2 Water flume:

The 40-ft. long water flume 30" wide and $3\frac{1}{2}$ ft. high provided a calm flow ahead of the test section. The maximum discharge was about 7 cfs circulated by a pumping system and stabilized by an overhead tank. The discharge was measured by an orifice flow meter and checked by a volumetric tank. A plate with holes and two steel meshes were used to keep the flow uniform.

To eliminate boundary layer effect, a parabolic entrance contraction was installed in the middle of the flume. This contraction was necessary to provide a high enough velocity. The velocity distribution in the 15" x 15" test section was checked by a miniature propeller current meter. The deviation of the velocity from average was ± 1.7%. Water depth in the test section was controlled by a tail gate. (Fig. 10). Critical flow was avoided by controlling the height of the tail water gate, because surface waves are a problem near critical depth. This condition limits the maximum velocity which we could use. A point gauge accurate to one hundredth of a foot was used for measurement of flow depth in the test section.

Water surface drop at the entrance of the test section was very smooth, and no standing wave appeared. Therefore fair uniformity of velocity and pressure distribution was predicted.

4.3 Model mounting

A 3/4" square steel cantilever provided a mounting of constant flexibility and known damping coefficient for the vibrating system - a circular cylinder 2" in diameter and one foot long. Later a 4" diameter cylinder was also used as a test body. At first the cantilever was clamped on to a 5" steel I-beam across the top of the flume. When the cylinder was subjected to even medium flows, the 5" beam vibrated in torsion. The torsional rigidity of the I-beam being found to be too small, another 5" I-beam was clamped vertically to the concrete ceiling beam and to the horizontal steel beam. To check the accuracy of measurements of strain in the cantilever, possible movement of the support was checked by dial gauge. The movement appeared negligible even under cantilever resonant conditions.

The total length of the cantilever system was 38 inches. The portion of the submerged square section was surrounded by a streamlined strut to eliminate the effect of form drag of the cantilever itself.

The cantilever as well as the cylinder was changeable; hence the flexibility of the structure as well as the natural frequency of the system could be varied in the tests. This gave different resonant velocities and frequencies, and different types of self-excited and forced vibration.

4.4 Instrumentation:

Since measurements of the frequency and the displacement of the test body were required, the oscillograph was used. The electrical current, which varied according to the mechanical changes in the strain gauge, was amplified and recorded by pen recorder (Fig. 37). In order to record lateral and longitudinal vibration simultaneously, two sets of strain gauges, amplifiers and pen recorders were used. The recorders accuracy was very high at low frequency: 0 to 20 cps. A wide variation of amplitude was permitted by changing attenuations. Three recording speeds were used: 5, 25 and 125 mm per second. A pen was provided for the purpose of marking the graph and this pen was activated simultaneously with the camera shutter, so that photographs could be synchronised with the vibration record (Fig. 38-39). White floats were spread on the surface of the flow so that the flow path could be photographed.

V. Test Procedure and Analysis

5.1 Calibrations

The discharge of the flow meter was calibrated by weighing tank. The rating curve shows the relation between discharge and flow meter readings.

The amplitude of the vibrating cylinder was calibrated directly by a dial gauge in the test position. The corresponding deflections were recorded simultaneously by pen recorder. Because the bending of the steel beam was within elastic range, and because the cantilever was oscillating in its fundamental mode, the amplitude was assumed to be proportional to the reading on the straln gauge.

Force calibration was done by applying a known pulling force on the test body while the recorder was operating. The elastic response force could then be calculated from the calibration curve. It should be stressed that near resonance the applied force and the cantilever response are not equal, there being a considerable amplification of response at resonance.

The frequency of free damped vibration in water was found by vibrating the testing body in position. The cylinder was displaced from its equilibrium in a longitudinal direction and when released it vibrated at its natural frequency. The amplitude of vibration steadily diminished because of the damping. The procedure was repeated for the lateral direction and it was found that the frequencies of lateral and longitudinal vibrations were the same. From these damping curves both the natural frequency and the damping coefficient, n, were determined (17) by the equation:

$$\frac{\delta_t}{\delta_{t+T}} = e^{nT}$$

where T: period of vibration and logarithmic decrement β:

$$\beta = \text{In}\,\frac{\delta_t}{\delta_{t+T}} = nT$$

By varying the rigidity of the elastic system, four conditions of different damping coefficients were used in the experiment.

5.2 Experimental results

Experiment was divided into the following parts, and listed in Table I - VIII:

1. 2" circular cylinder with 3/4" square steel cantilever.
2. 4" circular " " 3/4" " " " .
3. 2" circular " " 5/8" " aluminum " .
4. 4" circular " " 5/8" " " " .
5. 2" circular " " 3/4" " steel " and 1/16" diameter wire placed at four different positions, i.e. 0°, 22.5°, 45° and 67.5°.
6. 2" circular cylinder with 5/8" square aluminum cantilever and 1/8" diameter wire placed at two positions, i.e. 0° and 45°.

All tests were run at 0.3 fps velocity increments, from the lowest flow for which the recorder was sensitive, to the highest flow for which the flow in the test section was sufficiently sub-critical to avoid surface disturbances. The speed of the pen recorder was set to 5 or 25 mm per second for general runs and 125 mm per second for special runs.

For the runs with 2" diameter cylinder and steel cantilever, a longitudinal force was applied by a wheel mechanism to the testing body while the lateral amplide was very small. This gave additional stiffness in the longitudinal direction only. Frequency was recorded through a series of flows. Since this represented the lateral direction vibration only at small vibrating amplitude, the results are very close to stationary cylinder readings. These results were analysed and plotted with S vs R_e in Fig. 11. The points followed Strouhal's description and fell into the band zone reported by other authors (7).

TABLE I. 2" cylinder with 3/4" square section steel cantilever

$fn = fn' = 10.4$ cps $D = 0.167'$ $Vres = 9.0$ fps $V'res = 4.5$ fps $\nu = 1.13 \times 10^{-5}$ ft^2/sec

Flow Condition				Lateral Vibration only			Both lateral and longitudinal Vibration			Both lateral and longitudinal Vibration			Longitude			Lateral		
(1) Run No.	(2) Velocity V fps	(3) Relative velocity V/Vres	(4) Reynolds No. Re 10^4	(5) Frequency f cps	(6) Strauhal No. fD/V	(7) f/fn	(8) Frequency fy cps	(9) Strauhal No. fyD/V	(10) fy/fn	(11) Frequency fx cps	(12) Strauhal No. fxD/V	(13) fx/fn	(14) Amplitude ratio $\delta x/D$	(15) Drag ΔPx lb	(16) Coe. $\beta_{\Delta px}$	(17) Amplitude ratio $\delta y/D$	(18) Lift Py lb	(19) Coe. β_{py}
11	1.010	0.112	1.49	1.112	0.183	0.108	1.112	0.183	0.108	0	0	0				0.002	0.12	0.73
12	0.906	0.100	1.34	1.010	0.185	0.098	1.010	0.185	0.098	0	0	0				0.001	0.08	0.61
13	0.840	0.093	1.25	0.908	0.180	0.088	0.908	0.180	0.088	0	0	0				0.001	0.04	
14	0.752	0.084	1.11	0.812	0.180	0.078	0.812	0.180	0.078	0	0	0				0.001	0.04	
15	0.610	0.068	0.90	0.680	0.185	0.066	0.680	0.185	0.066	0	0	0						
16	0.511	0.057	0.76	0.529	0.172	0.052	0.529	0.172	0.052	0	0	0						
17	1.450	0.160	2.14	1.600	0.184	0.155	1.600	0.184	0.155	0	0	0				0.005	0.30	0.89
18	2.180	0.242	3.21	2.290	0.175	0.222	2.29	0.175	0.222	0	0	0				0.013	0.75	0.96
20	2.280	0.252	3.37	2.56	0.185	0.248	2.56	0.185	0.248	10.4	0.755	1.0	0.035	2.14	2.54	0.029	1.77	2.09
21	2.530	0.280	3.74	2.64	0.174	0.256	8.40	0.550	0.815	10.4	0.670	1.0	0.079	5.00	4.81	0.055	3.25	3.13
22	2.890	0.320	4.27	3.25	0.186	0.316	10.25	0.588	1.00	10.4	0.595	1.0	0.103	6.43	4.83	0.053	3.20	2.41
23	3.27	0.361	4.82	3.76	0.191	0.365	10.35	0.526	1.00	10.5	0.525	1.0	0.143	8.92	5.17	0.038	2.30	1.34
24	3.62	0.400	5.34	4.02	0.185	0.390	10.40	0.478	1.00	10.3	0.476	1.0	0.169	10.30	4.86	0.049	2.90	1.37
25	3.99	0.442	5.89	4.52	0.180	0.439	9.00	0.375	0.874	10.5	0.430	1.0	0.178	11.40	4.42	0.062	3.70	1.43
26	4.35	0.482	6.43	5.55	0.211	0.539	5.93	0.226	0.575	10.5	0.397	1.0	0.095	5.35	1.74	0.075	4.50	1.46

TABLE II. 2" cylinder with 3/4" square section steel cantilever and wire in place

$f_n = f_n' = 10.4$ cps $V_{res} = 9.0$ fps $V_{res}' = 4.5$ fps $D = 0.167'$

(1) Run No.	(2) Wire placed at	(3) V fps	(4) $\frac{V}{V_{res}}$	(5) $\frac{Re}{10^4}$	(6) f	(7) $\frac{fD}{V}$	(8) f/f_n	(9) δ in	(10) fy	(11) f_y/f_n	(12) $\frac{f_yD}{V}$	(13) fx	(14) $\frac{f_x}{f_n}$	(15) $\frac{f_xD}{V}$	(16) δ_x in	(17) δ_x/D	(18) δ_y in	(19) δ_y/D
37		2.18	0.24	3.21	2.80	0.214	0.272	0.008	2.8	0.272	0.214	0	0	0	0	0	0.010	0.005
35		2.53	0.28	3.74	3.56	0.234	0.343	0.018	10.4	1.0	0.682	10.4	1.0	0.755	0.116	0.058	0.170	0.085
38		2.89	0.32	4.27	3.94	0.227	0.382	0.021	10.4	1.0	0.597	10.4	1.0	0.670	0.233	0.117	0.184	0.092
36	45°	3.27	0.36	4.82	4.52	0.230	0.439	0.026	10.4	1.0	0.528	10.4	1.0	0.595	0.405	0.203	0.110	0.055
39		3.62	0.40	5.34	4.90	0.227	0.472	0.034	10.4	1.0	0.478	10.4	1.0	0.525	0.452	0.226	0.084	0.043
40		3.99	0.44	5.89	6.31	0.264	0.612	0.036	7.8	0.75	0.326	10.4	1.0	0.476	0.452	0.226	0.170	0.083
41		4.35	0.48	6.43	7.30	0.279	0.708	0.031	6.3	0.61	0.241	10.4	1.0	0.430	0.135	0.068	0.170	0.085
46		2.18	0.24	3.21	2.44	0.186	0.237	0.021	2.5	0.24	0.191	10.4	1.0	0.798	0.028	0.014	0.025	0.013
47		2.53	0.28	3.74	2.96	0.195	0.287	0.038	9.2	0.885	0.602	10.4	1.0	0.755	0.165	0.083	0.037	0.019
44		2.89	0.32	4.27	3.52	0.202	0.342	0.032	10.4	1.0	0.663	10.4	1.0	0.670	0.172	0.086	0.116	0.058
48	67.5°	3.27	0.36	4.82	3.92	0.199	0.381	0.045	10.4	1.0	0.531	10.4	1.0	0.595	0.295	0.148	0.061	0.031
45		3.62	0.40	5.34	4.10	0.188	0.398	0.037	10.4	1.0	0.478	10.4	1.0	0.525	0.306	0.153	0.110	0.055
49		3.99	0.44	5.89	4.26	0.178	0.413	0.030	6.5	0.625	0.270	10.4	1.0	0.476	0.485	0.243	0.177	0.088
50		4.35	0.48	6.43	5.00	0.195	0.485	0.025	5.5	0.530	0.210	10.4	1.0	0.430	0.300	0.150	0.178	0.089

TABLE II. Continued

(1) Run No.	(2) Wire placed at	(3) V fps	(4) $\frac{V}{Vres}$	(5) $\frac{Re}{10^4}$	(6) f	(7) $\frac{fD}{V}$	(8) f/fn	(9) δ in	(10) fy	(11) fy/fn	(12) $\frac{fyD}{V}$	(13) fx	(14) $\frac{fx}{fn}$	(15) $\frac{fxD}{V}$	(16) δx in	(17) $\delta x/D$	(18) δy in	(19) $\delta y/D$
51	22.5°	2.18	0.24	3.21	2.07	0.158	0.201	0.032	2.07	0.201	0.158	0	0	0	0	0	0.030	0.015
52		2.53	0.28	3.74	2.68	0.176	0.260	0.048	5.60	0.540	0.367	10.4	1.0	0.755	0.092	0.046	0.080	0.040
42		2.89	0.32	4.27	2.92	0.168	0.283	0.075	8.50	0.816	0.488	10.4	1.0	0.670	0.165	0.083	0.122	0.061
53		3.27	0.36	4.82	3.34	0.170	0.324	0.115	10.4	1.0	0.528	10.4	1.0	0.595	0.160	0.080	0.160	0.080
43		3.62	0.40	5.34	3.80	0.175	0.369	0.110	10.4	1.0	0.478	10.4	1.0	0.525	0.257	0.128	0.227	0.114
54		3.99	0.44	5.89	4.06	0.169	0.394	0.080	10.4	1.0	0.345	10.4	1.0	0.476	0.307	0.154	0.184	0.092
55		4.35	0.48	6.43	4.20	0.160	0.408	0.114	10.4	1.0	0.398	10.4	1.0	0.430	0.355	0.178	0.215	0.108
56	0°	2.18	0.24	3.21	2.36	0.180	0.227	0.031	10.4	1.0	0.796	10.4	1.0	0.798	0.068	0.034	0.086	0.043
57		2.53	0.28	3.74	2.86	0.187	0.275	0.055	10.4	1.0	0.683	10.4	1.0	0.755	0.116	0.058	0.120	0.060
58		2.89	0.32	4.27	3.42	0.196	0.329	0.043	10.4	1.0	0.597	10.4	1.0	0.670	0.165	0.083	0.141	0.071
59		3.27	0.36	4.82	3.76	0.191	0.362	0.040	3.60	0.346	0.183	10.4	1.0	0.595	0.153	0.087	0.120	0.060
60		3.62	0.40	5.34	4.06	0.186	0.390	0.061	4.06	0.390	0.186	0	0	0	0.037	0.019	0.074	0.037
61		3.99	0.44	5.89	4.3	0.179	0.413	0.055	4.30	0.413	0.179	0	0	0	0.025	0.013	0.055	0.028
62		4.35	0.48	6.43	5.1	0.195	0.490	0.123	5.10	0.490	0.194	0	0	0	0.037	0.019	0.120	0.060

TABLE III. 4" cylinder with 3/4" square steel cantilever

$f_n = f_n' = 6.5$ cps Vres = 11.8 fps Vres' = 5.9 fps D = 0.334'

(1) Run No.	(2) V fps	(3) V/Vres	(4) Re/10^4	(5) fx	(6) fx/fn	(7) Sx	(8) fy	(9) fy/fn	(10) Sy	(11) δx	(12) $\delta x/D$	(13) ΔPx	(14) $\beta_{\Delta P_x}$	(15) δy	(16) $\delta y/D$	(17) Py	(18) β_{Py}
70	1.78	0.153	5.26	0	0	0	1.07	0.164	0.200	0	0	0	0	0.019	0.005	0.582	1.13
71	2.14	0.183	6.34	0	0	0	1.28	0.195	0.239	0	0	0	0	0.049	0.012	1.45	1.94
73	2.48	0.213	7.32	6.5	1.0	0.871	1.66	0.254	0.317	0.025	0.006	0.60	0.601	0.055	0.014	1.53	1.52
74	2.85	0.244	8.45	6.5	1.0	0.763	2.60	0.397	0.464	0.147	0.038	4.30	3.22	0.116	0.029	3.37	2.54
75	3.22	0.275	9.53	6.5	1.0	0.679	3.00	0.458	0.475	0.171	0.043	5.00	2.96	0.153	0.038	4.48	2.66
76	3.56	0.305	10.50	6.5	1.0	0.610	3.40	0.520	0.486	0.074	0.019	2.15	1.05	0.110	0.028	3.20	1.54
77	3.91	0.336	11.60	6.5	1.0	0.552	4.00	0.610	0.518	0.074	0.019	2.15	0.865	0.153	0.038	4.48	1.80
78	4.28	0.367	12.70	6.5	1.0	0.506	5.20	0.795	0.615	0.098	0.027	2.85	0.955	0.110	0.028	3.20	1.70

TABLE IV. 2" cylinder with 5/8" square aluminum cantilever

fn = fn = 4.5 cps Vres = 4.0 fps V'res = 2.0 fps $\beta p_y = \dfrac{Py}{A\rho \frac{V^2}{2}}$ $\beta_{\Delta} p_x = \dfrac{\Delta Px}{A\rho \frac{V^2}{2}}$

(1) Run No.	(2) V fps	(3) V/Vres	(4) Re 10^4	(5) fx	(6) fx/fn	(7) Sx	(8) fy	(9) fy/fn	(10) Sy	(11) y in	(13) Py lb	(14) β_{p_y}	(15) δ_x in	(16) ΔPx lb	(17) $\beta_{\Delta P_x}$
101	0.752	0.186	1.11	0	0	0	0.83	0.190	0.184	0.010	0.055	0.595	0	0	0
102	1.090	0.271	1.61	4.5	1.0	0.776	1.30	0.290	0.198	0.091	0.445	2.060	0.167	0.823	4.26
103	1.450	0.361	2.14	4.5	1.0	0.585	4.50	1.00	0.517	0.025	0.123	0.360	0.243	1.200	3.50
104	1.810	0.450	2.68	4.5	1.0	0.467	2.75	0.610	0.504	0.0625	0.308	0.580	0.389	1.920	3.50
105	2.180	0.486	3.21	4.5	1.0	0.388	2.40	0.535	0.183	0.311	1.53	1.970	0.365	1.800	2.33
106	2.530	0.632	3.74	4.6	1.02	0.338	2.55	0.567	0.168	0.770	3.83	3.670	0.348	1.700	1.63
107	2.890	0.722	4.27	4.7	1.04	0.304	3.35	0.745	0.192	0.987	4.85	3.560	0.097	0.480	0.35
108	3.270	0.814	4.82	4.9	1.09	0.286	3.35	0.745	0.171	1.83	9.05	5.220	0.070	0.340	0.20
109	3.620	0.902	5.34				3.50	0.778	0.161	2.39	11.80	5.550	0.084	0.410	0.20
110	3.990	0.992	5.89				3.78	0.840	0.159	3.31	15.30	5.920	0.416	2.050	0.80
111	4.350	1.080	6.43				3.92	0.872	0.151	3.53	17.40	5.630	0.450	2.100	0.681

TABLE V. 2" cylinder with 5/8" square section aluminum cantilever and wire in position

$f_n = f'_n = 4.5$ cps $V_{res} = 4.0$ fps $V'_{res} = 2.0$ fps

(1) Run No.	(2) Wire placed at	(3) V fps	(4) $\frac{V}{V_{res}}$	(5) $\frac{Re}{10^4}$	(6) f_y	(7) f_y/f_n	(8) f_yD/V	(9) f_x	(10) f_x/f_n	(11) f_xD/V	(12) δ_x	(13) δ_x/D	(14) δ_y	(15) δ_y/D
115	45°	0.752	0.187	1.11	0.91	0.202	0.202	0	0	0	0	0	0.007	0.004
116		1.090	0.272	1.61	1.36	0.302	0.208	0	0	0	0.010	0.005	0.011	0.006
117		1.450	0.361	2.14	4.50	1.00	0.218	4.5	1.00	0.515	0.232	0.116	0.118	0.059
118		1.810	0.450	2.68	2.30	0.512	0.212	4.7	1.04	0.430	0.056	0.028	0.118	0.059
119		2.180	0.542	3.21	2.35	0.523	0.180	4.6	1.02	0.350	0.196	0.098	0.360	0.180
120		2.53	0.632	3.74	3.10	0.690	0.204	4.5	1.00	0.296	0.323	0.162	0.514	0.257
121		2.89	0.722	4.72	4.00	0.890	0.229	4.5	1.00	0.259	0.120	0.060	1.010	0.505
123		3.62	0.902	5.34	4.25	0.945	0.195	4.5	1.00	0.206	0.348	0.174	2.780	1.390
125		4.35	1.080	6.43	4.85	1.080	0.186	4.5	1.00	0.172	0.243	0.122	2.090	1.045
130	0°	0.752	0.187	1.11	0.80	0.180	0.178	0	0	0	0	0	0.011	0.006
131		1.450	0.361	2.14	1.48	0.330	0.170	0	0	0	0.010	0.005	0.097	0.049
132		2.180	0.542	3.21	2.12	0.471	0.162	4.2	0.94	0.319	0.091	0.046	0.415	0.208
133		2.890	0.722	4.72	3.92	0.651	0.225	4.2	0.94	0.241	0.007	0.004	1.670	0.835
134		3.62	0.902	5.34	4.78	1.060	0.220	4.2	0.94	0.192	0.208	0.104	2.920	1.460
135		4.35	1.080	6.43	4.67	1.040	0.178	4.2	0.94	0.160	0.208	0.104	2.780	1.390

TABLE VI. 4" cylinder with aluminum 5/8" square section cantilever

$f_n = f_n' = 2.8$ cps $V_{res} = 5.1$ fps $V_{res}' = 2.6$ fps

(1) Run No.	(2) V fps	(3) $\frac{V}{V_{res}}$	(4) $\frac{Re}{10^4}$	(5) f_y	(6) f_y/f_n	(7) $\frac{f_y D}{V}$	(8) f_x	(9) $\frac{f_x}{f_n}$	(10) $\frac{f_x D}{V}$	(11) δ_y in	(12) $\frac{\delta_y}{D}$	(13) P_y lb	(14) β_{P_y}	(15) δ_x in	(16) $\frac{\delta_x}{D}$	(17) ΔP_x lb	(18) $\beta_{\Delta P_x}$
79	0.74	0.144	2.18	0.43	0.154	0.20	0	0	0	0.014	0.004	0.069	0.78	0	0	0	0
80	1.07	0.210	3.15	0.58	0.207	0.18	0	0	0	0.036	0.009	0.178	0.95	0	0	0	0
81	1.43	0.279	4.20	0.69	0.246	0.16	2.8	1.0	0.672	0.470	0.118	1.16	3.49	0.390	0.098	1.89	6.11
82	1.24	0.242	3.69	0.63	0.225	0.17	2.8	1.0	0.794	0.256	0.064	1.26	5.00	0.250	0.062	1.21	5.15
83	1.17	0.229	3.50	0.62	0.222	0.18	2.8	1.0	0.815	0.110	0.028	0.548	2.44	0.153	0.038	0.74	3.55
84	1.78	0.348	5.26	0.96	0.343	0.18	2.8	1.0	0.520	0.612	0.153	1.50	2.91	0.700	0.175	3.37	7.02
85	2.14	0.419	6.34	1.15	0.411	0.17	2.9	1.03	0.436	0.808	0.202	3.97	4.01	1.150	0.288	5.56	8.05
86	2.48	0.487	7.32	1.46	0.522	0.19	2.9	1.03	0.372	1.26	0.315	6.23	6.24	0.975	0.244	4.71	5.07
87	2.85	0.557	8.45	2.15	0.768	0.25	2.8	1.0	0.325	1.57	0.392	8.55	6.42	0.236	0.059	1.15	0.94
88	3.22	0.629	9.53	2.47	0.882	0.26	2.8	1.0	0.290	2.37	0.592	11.60	6.88	0.220	0.055	1.10	0.71
89	3.56	0.695	10.50	2.66	0.950	0.25	0	0	0	3.56	0.890	17.50	8.45	0.139	0.035	0.69	0.35
90	3.91	0.768	11.60	2.72	0.970	0.23	0	0	0	3.73	0.932	18.40	7.35	0.167	0.042	0.82	0.35
91	4.28	0.836	12.70	2.77	0.990	0.22	0	0	0	3.95	0.990	19.50	6.54	0.110	0.023	0.55	0.20

TABLE VII

Natural frequency of free damped vibration in water:

Material	Cylinder diameter	β	N	Natural frequency fn cps	$fn/2$
Steel	2"	0.0567	0.590	10.4	5.2
Steel	4"	0.0414	0.269	6.5	3.3
Aluminum	2"	0.0961	0.432	4.5	2.3
Aluminum	4"	0.111	0.312	2.8	1.4

TABLE VIII

Velocity of resonance (based on the assumption: fx = 2fy)

Material	Cylinder diameter	Vres fps	$V'res$ fps	Rres 10^4	$R'res$ 10^4
Steel	2"	9.0	4.5	13.2	6.6
Aluminum	2"	4.0	2.0	5.9	2.9
Steel	4"	11.8	5.9	34.5	17.3
Aluminum	4"	5.1	2.6	15.0	7.5

For further study of the relationship between longitudinal and lateral vibrations, a series of runs were done. They showed how the longitudinal fibration was developed. First, as above, the lonitudinal vibration was suppressed (see Fig. 5 - 7), and the oscillogram recorded was a straight line in the longitudinal direction, i.e. there was stationary drag alone. Simultaneously a sinusoidal oscillating curve was recorded in the lateral direction. This curve belonged to the forced vibration category. Then, the suppressing force in the longitudinal direction was removed and vibration in the longitudinal direction was built up. With the development of longitudinal self-excited vibration, the lateral vibrating curves changed in shape. At the beginning, the lateral curve was distorted, in that it was sharper in shape and wavy along the rising or descending limbs. Later, when the self-excited longitudinal vibration reached its maximum, the lateral curve became irregular with larger amplitude and indicated vibration in a resonant condition. This also gave an explanation (Fig. 19 - the variation of vibrating types) of the curves with ordinates $\frac{f}{f_n}$ vs $\frac{V}{V_{res}}$. In these curves longitudinal resonance occured at $\frac{V}{V_{res}} = 0.30$ to 0.5. Owing to the effect of resonance in longitudinal direction, the points of lateral frequency moved away from the line of forced vibration. Since the motion of the vibrating system changed, it was called controlled vibration.

The frequency of lateral vibration giving an irregular oscillogram was analysed by counting the upward limbs which crossed the mean level of the oscillogram.

5.3 Analysis of experimental data

<u>Frequency</u>: there were three different conditions under which the frequency was measured:

1) Frequency of lateral vibration alone (f): i.e. with longitudinal vibration suppressed. The results approached those obtained in the stationary cylinder condition, if the amplitude was small. (Table I, column 5).
2) Lateral frequency of vibration for both x, y directions vibration (f_y): this frequency varies with lateral as well as the longitudinal vibration. (Table I, column 8).
3) Longitudinal frequency of vibration for both x, y direction vibration (f_x): this frequency curve was regular in shape and belonged to the category of self-excited vibration. (Table I, column 11).

For the purpose of analysis, Strouhal number for variations of eadh of the above types were calculated, as were the frequency ratios $^f/_{f_n}$.

In the range of $R_e = 5 \times 10^3 - 3 \times 10^5$, Strauhal Number is almost constant. The following relation can be obtained

$$\frac{f_s D}{V} = S = S_{res} = \frac{f_n D}{V_{res}}$$

$$\therefore \quad \frac{V}{V_{res}} = \frac{f_s}{f_n}$$

The above expression is a straight line inclined 45° to the horizontal (Fig. 19 - 23), representing the forced vibration due to the excitation of the eddy shedding force on a stationary cylinder.

<u>Amplitude</u>: The lateral and longitudinal amplitudes were analysed separately.

1) Lateral Amplitude: this was the amplitude when lateral and longitudinal vibration both took place. The maximum value was selected from the recording oscillograms.
2) Longitudinal Amplitude: only the maximum value was analysed because it varied only within a small range, i.e. the shape of the vibrating curve was more regular than in the case of lateral vibration.

Both of these were in dimensionless form $^{\delta}/_{D}$.

With the data, amplitude ratio vs R_e curves (Fig. 24 - 30) were plotted. Relation between the longitudinal and lateral amplitude variation was shown in the figures.

Forces: Forces in two directions - drag and lift - were calculated. There were the vibrating drag and lift which were additional to the steady drag and lift. For the sake of comparison, the dynamic energy of the uniform flow was used as a standard base for both response coefficients of vibrating drag and lift calculations.

Velocity of resonance: the velocity of uniform approaching flow, when the vibration of the cylinder system was at resonance, was the velocity of resonance. Because there were two resonances which could occur, two velocities of resonance existed. Lateral resonance happened at the frequency of eddy shedding, which coincided with the natural frequency in the lateral direction. Similarly longitudinal resonance occurred at longitudinal natural frequency.

Before longitudinal resonance the longitudinal response will exist in same phase with the oscillating drag. When the frequency of longitudinal excitation approaches natural frequency of the elastic system, the structure will vibrate near natural frequency. Then the amplitude keeps increasing to its maximum. Theoretically the longitudinal resonance velocity is one half that of lateral. But due to the distorsion of vortex, and the interaction of two-dimensional effects the experiment resulted that $^{V}res/_{V_{res}}$ was about 0.4.

From the relation between the velocity of the uniform flow and the eddy shedding frequency under the condition of stationary cylinder (Fig. 18) the assumed velocities of resonance for both lateral and longitudinal directions were selected and listed in Table VIII.

VI. Discussion of Results and Conclusion

6.1 Discussion:

Frequency: The Strouhal number is nearly constant when the Reynolds' number is in the range of 10^3 10^5 for a stationary cylinder. But, in two-dimensional vibration, when vibration is excited in the longitudinal direction, the Strouhal number of the lateral direction suddenly increases. The peak of this steep curve approaches S_x vs R_e curve as a tengent line. After the peak, the S_y value drops and merges into the band region (Fig. 11) given by the stationary cylinder tests. The shape of the rising curve depends upon several variables: k, spring constant; f'_n, natural frequency in longitudinal direction; and n, elastic and viscous damping coefficient.

The starting point of the shear layer is important for the generation of vortex shedding. If one of these separation points is fixed at one side of the cylinder and the one at the other side is left free to move during vibration, the balanced periodic oscillating force will be altered, as will the periodic circulation variation. Therefore when this vortex starter wire is in position, the separation point is controlled by the location of the wire. Then the beginning of the shear layer also changes its location, and non-balanced shear layers give a different eddy generating condition. This unbalanced force condition affects the exciting forces, also the frequency of vibration and the Strouhal Number as well. (Fig. 15 and 16). The magnitude of the Strouhal Number will be the highest when the wire is placed at a 45° position. Then the next ones are that when the wires are placed at positions 67.5°, 0°, 22.5°, and finally no wire condition. The lowest S occurs with the wire at 22.5°. When there is vibration in both directions,

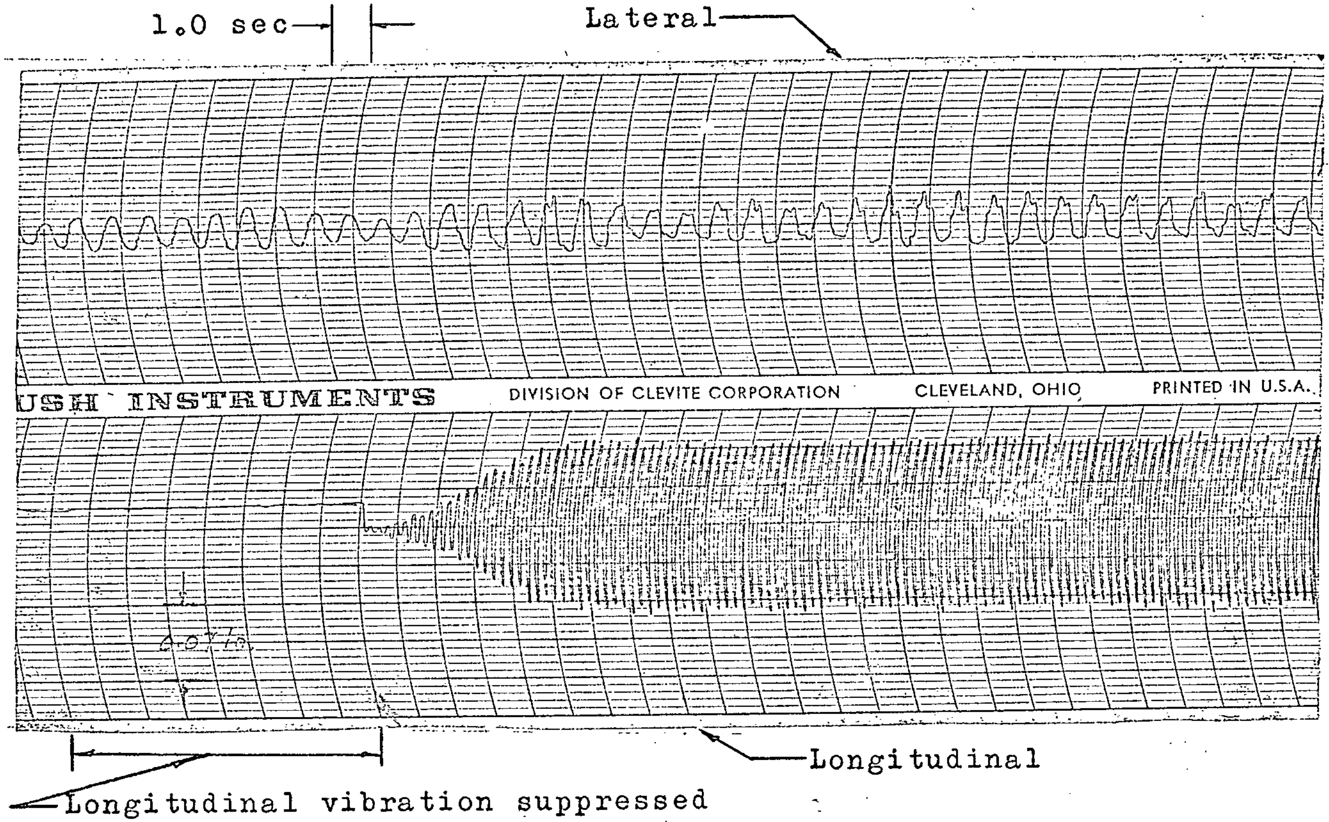

U = 1.09fps
2"cylinder, aluminum cantilever

Fig. 5 Development of longitudinal vibration

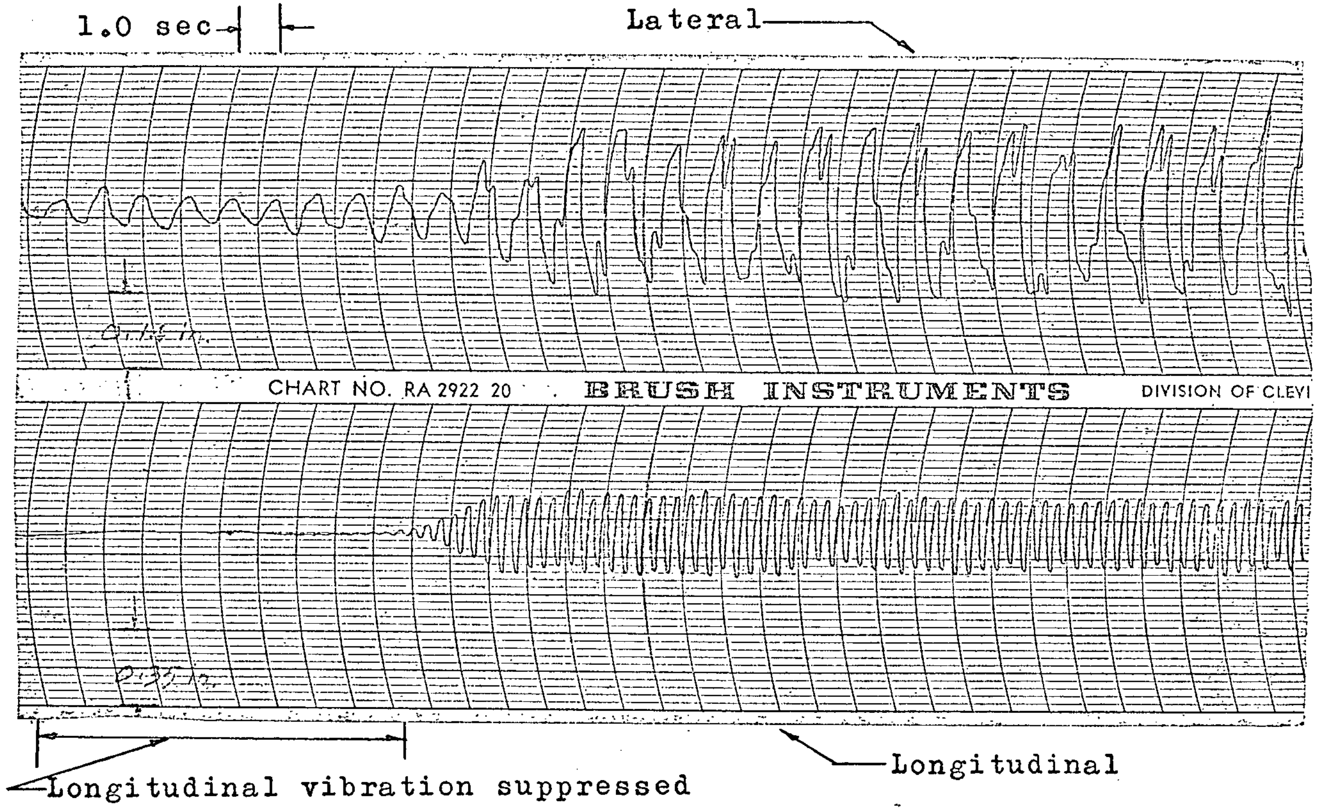

U = 1.45 fps
4" cylinder, aluminum cantilever

Fig. 6 Development of longitudinal vibration

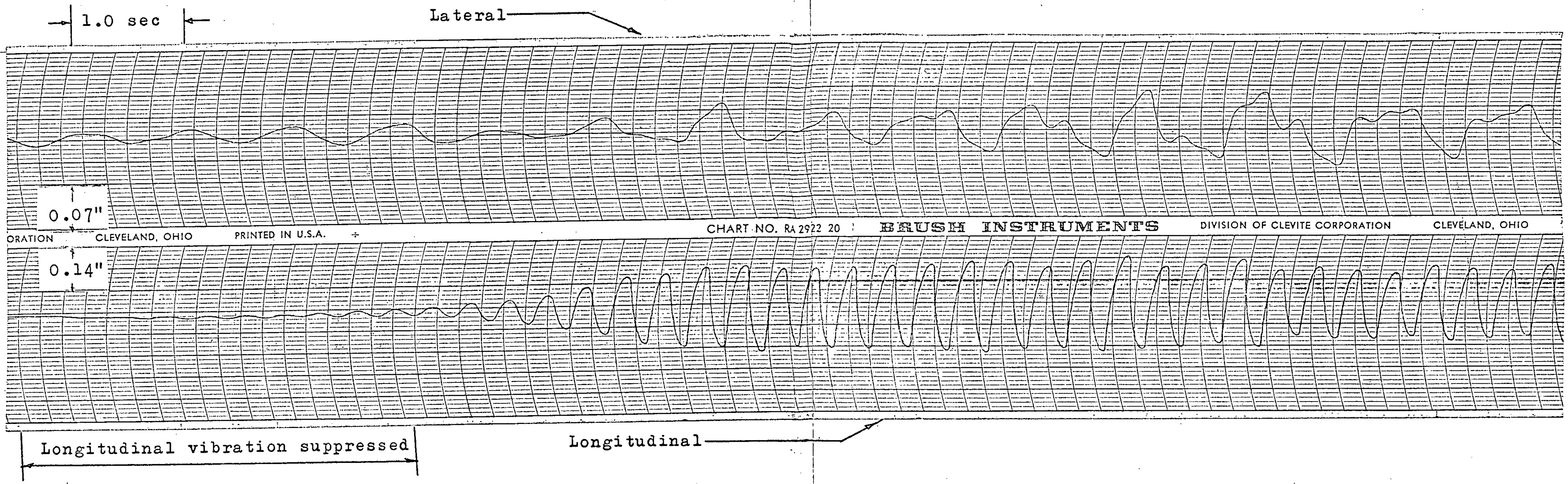

U = 1.81 fps
4" cylinder, aluminum cantilever

Fig. 7 Distorsion of lateral oscillogram the Strouhal Number variation is quite complex. An additional longitudinal effect makes the curve (S vs R_e) distorted. But it still bears the characteristics of combined effects.

The relation of frequency ratio vs velocity ratio describes the type of vibration to be expected in the test. (Fig. 19). At low flows the amplitude is small and the velocity is far from the velocity of resonance for both longitudinal and lateral directions. It is in forced vibration. As soon as the velocity ratio increases to near 0.3, the longitudinal vibration starts, and the lateral vibration is gradually changed by longitudinal resonance. The points in this region appear on the diagram as controlled vibration. When the velocity ratio approaches 0.7, the longitudinal vibration disappears, and the curve of the controlled lateral vibration drops back and coincides with that of forced vibration. This depends on the value of the natural frequency and the magnitude of spring constant. If the natural frequency in lateral direction is small, the difference between the natural frequencies in longitudinal and lateral direction is also small. This means that the resonant regions are too close to each other, and the variation on the graph is not obvious. If spring constant is small, the amplitude around longitudinal resonance will be too large so that, due to the fast shifting of separation points and the increasing rate of eddy generation, the flow pattern at rear part of the cylinder becomes almost random. The character of the vibration then alters.

In Fig. 19 to Fig. 23, the types of vibration are shown. Because the maximum attainable flow was limited by flume flow conditions, some points near lateral resonance were not attainable.

<u>Amplitude</u>: the amplitude ratio for longitudinal direction suddenly rises to its peak near the point of longitudinal resonance and then falls to a very

small magnitude. But the lateral amplitude ratio, when the longitudinal one reaches a peak, rises slowly first, then drops and passes through a minimum value in the region of longitudinal resonance. Then it rises again toward the condition where lateral vibration only exists.

The largest amplitude ratio of longitudinal vibration in these four sets of tests is about 0.25, near a velocity ratio of 0.4. When the wires were in position, all the maximum values were in the region of velocity ratio about 0.4.

Response coefficient of oscillating lift and drag of an elastic body

The response coefficient of vibrating lift and drag due to an oscillating fluid force is computed by the following equations:

$$B_{\Delta px} = \frac{\Delta P_x}{A \rho U^2/2}$$

$$B_{py} = \frac{P_y}{A \rho U^2/2}$$

The vibrating lift varies with the rigidity of the structure. Its maximum values occur between velocity ratio 0.2 and 0.4 in the region of longitudinal effect. The response coefficient of vibrating lift have a value above 3 for 2" cylinder and steel cantilever (Fig. 31).

The maximum vibrating drag response coefficient occurs in the region when the velocity ratio is between 0.2 to 0.5, and its magnitude is about 5 to 8 in these test runs for the damping coefficients (n value) in the range of 0.25 to 0.60.

6.2 Conclusion

1) The self-excited longitudinal vibration occurs between the velocity ratio of 0.2 to 0.8, when both x and y directions are allowed to vibrate. Its peak is around 0.4. The frequency of oscillating drag, which is the

excitation force of longitudinal vibration near longitudinal resonance, is predicted to be twice that of the lateral oscillating lift.

2) In the region of longitudinal resonance, the oscillogram is affected and distorted in the lateral direction by longitudinal vibration. The degree of distortion depends on the amplitude of the longitudinal vibration. Hence, the frequency of lateral vibration increases with the intensity of longitudinal vibration. This is referred to as a controlled vibration.

3) The Strouhal Number of lateral vibration reaches a peak (Fig. 11) in the region of longitudinal resonance and approaches the curve: S_x vs R_e as a tangent.

4) Lateral vibration in two-dimensional vibration is neither the self-excited nor the forced type. It is affected by longitudinal movement, and is therefore called controlled vibration.

5) In two-dimensional vibration, the amplitude of longitudinal vibration in the region of longitudinal resonance rises suddenly to a peak and then decreases again to a very low value.

6) In two-dimensional vibration, the amplitude of lateral vibration in the region of longitudinal resonance first rises and then decreases to a lower value as longitudinal amplitude approaches its maximum. Then the curve rises again to the original path which is the characteristic of lateral vibration alone.

7) When the separation point is controlled by wire location, the starting point of the shear layer is altered. Hence the periodic excitation of the vibrating lift and drag is altered. The unsymmetrical oscillating fluid forces produce an oscillogram with irregular shape and change the vibrating frequency, sometimes decreasing the amplitude of vibration and sometimes increasing it. At present no general conclusion concerning the best position of the starter wire has been possible.

8) The response coefficient of vibrating lift due to oscillating fluid force is about 5 in these four conditions of different spring constant, damping constant and natural frequency values. The peaks appear at $\frac{V}{V_{res}}$ = 0.2 to 0.5. For vibrating drag it varies from 3 to 8 in the region of longitudinal resonance.

9) There would be a second maximum for amplitude of lateral vibration at or near a velocity ratio of 1.0 but only one test was run in this range (Fig. 21). Around this region the vibration appeared to be a controlled type.

10) Because the longitudinal vibration appeared at a velocity ratio as low as about 0.4, the design of hydraulic structures in this region of flow should be checked for the instability arising from two-dimensional vibration, if the structure allows to vibrate.

APPENDIX I

Structural Vibration

When a structure is acted by an external disturbance the forced vibration will take place. The forces that come into play will be external force, inertia force, elastic restoring force of the structural system and damping forces. When simplified as a problem of a single concentrated mass, the equation will be in the form (17):

$$M\ddot{x} + D\,(t) + kx = F\,(t)$$

Under the assumptions that the pulsating load: $F\,(t) = F_o \operatorname{Sin} \omega t$ and the viscous damping: $D\,(t) = cx$ by ignoring transient solution, the particular solution will be:

$$x_p = \Delta H \left[\left(1 - \left(\frac{\omega}{p}\right)^2\right) \operatorname{Sin} \omega t - \frac{2\,n\omega}{p^2} \operatorname{Cos} \omega t \right]$$

where $$H = \frac{1}{\left[1 - \left(\frac{\omega}{p}\right)^2\right]^2 + \frac{4n^2\,\omega^2}{p^4}}$$ (called: magnification factor)

The characteristic of vibrating motion can be expressed by relation between H and $\omega/_p$:

where: p = circular frequency

ω = angular velocity

n = $c/_{2M}$

Δ = static deflection

It says when frequency of disturbing force approaches natural frequency the amplitude will be the maximum under the energy balance of disturbing and damping forces.

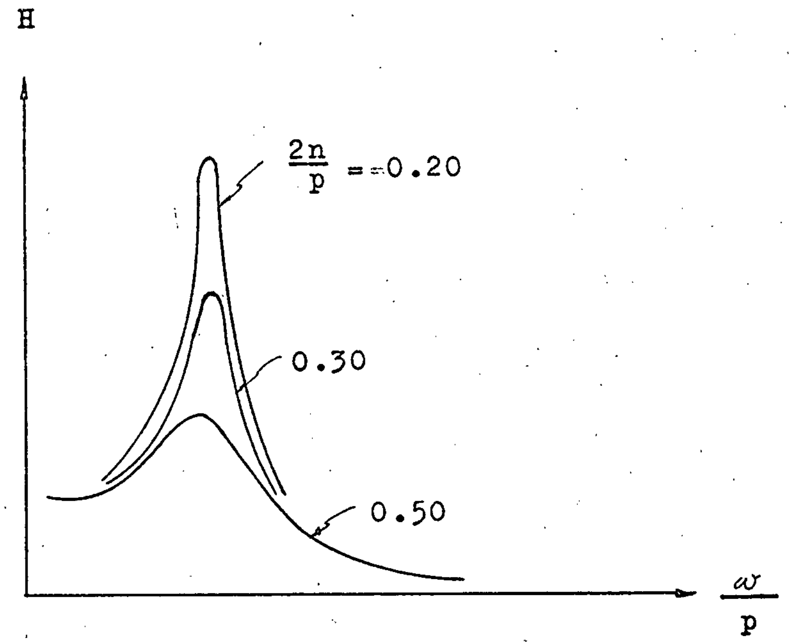

Fig. 8 Resonance of structural vibration

The force vibration of an elastic slender beam of continuous mass distribution is governed by the equation:

$$EI \frac{\partial^4 y}{\partial x^4} + M \frac{\partial^2 y}{\partial t^2} = F(t)$$

where $F(t) = C_K \cdot q \cdot \sin \omega t$ if external sinusoidal force is the lift caused by a fluid flow.

The solving of the homogenious boundary problem diferential equation, i.e. let the $F(t) = 0$, yields the solution of natural frequency of the slender, elastic beam:

$$f = c \sqrt{\frac{EI}{ML^4}}$$

where: c is a coefficient depends on the type of beam and mode of vibration .

m: mass per unit length ..

APPENDIX II

Quasi-Steady Theory

Because of no complete hydrodynamic theory for the separated flow the quasi-steady (semiempirical theory) is employed. Using stationary hydrodynamic forces on a vibrating body, a solution is obtained for a non-linear differential equation. If the fluid force in the forced vibration equation is:

$$F_y = C \frac{\rho}{2} A U^2 \qquad \text{(Lateral force)}$$

where: $C = f(\alpha, C_L, C_D)$

Then with a simplified relation, using a polynomial to express the function of coefficient of lift and drag, the resulting equation will be (15):

$$\ddot{Y} - e\,(1 - P\,\dot{Y}^2 - Q\,\dot{Y}^4)\,\dot{Y} + Y = 0$$

where Y is a dimensionless displacement, and e, p and Q are damping constants. A solution, involving the substitution of polynomial approximations to the aerodynamic force curve, has been used to predict approximately the amplitude of the vibration.

Bibliography

1. L. Rosenhead: Laminar Boundary Layers, p. 93, 102. Oxford, 1963.

2. M. Rauscher: Introduction to Aeronautical Dynamics, p. 25, 257, 366, John Wiley, 1953.

3. W. Kaufmann: Fluid Mechanics, p. 251, 257, McGraw Hill, 1963.

4. V.L. Streeter: Fluid Dynamics, Chap. VII, p. 200.

5. D.M. McGrefor: An Experimental Investigation of the Oscillating Pressures on a Circular Cylinder in a Fluid Stream. U. of Toronto, 1957.

6. W. Weaver: Wind Induced Vibrations in Anttenna Members. Trans. Vol. 127, 1962, ASCE, p. 681.

7. Eduard Naudascher: On the Role of Eddies in Flow-induced Vibrations Iowa Institute of Hydraulic Research; I.A.H.R. Congress, London, (1963 sep.).

8. G.H. Toebes: Hydroelastic Forces on Hydraulic Structures due to Turbulent Wake Flows, Purdue University. I.A.H.R. Congress, Dubrovnik, 1961.

9. A. Laird: Water Eddy Forces on Oscillating Cylinder, A.S.C.E. Trans. 1962.

10. J.H. Gerrard: An Experimental Investigation of Oscillating Lift and Drag, J. of Fluid Mechanics, 1961.

11. Eduard Naudashcher: Vibration of Gates During Overflow and Underflow, A.S.C.E. Trans. 1962.

12. F.B. Campbell: Vibration Problem in Hydraulic Structure. A.S.C.E. Trans. 1962.

13. A. Laird: Groups of Vertical Cylinder Oscillating in Water, J. of Eng. Mechanics, Feb., 1963.

14. D. Pierce: Photographic Evidence of Formation and Growth of Vorticity, J. of Fluid Mechanics, 1961.

15. G.V. Parkinson: On the Aeroelastic Instability of Bluff Cylinders, A.S.M.E., J. of Applied Mechanics, June 1962.

16. A. Roshko: Experiments on Flow Past a Circular Cylinder at very High Reynold's Number, May 1961, J. of Fluid Mechanics.

17. Rrover: Dynamics of Frame Structure.

18. Norris: Structural Design for Dynamic Load.

19. Birhoff: Jets, Wakes and Cavities.

20. H. Sato: Mechanism of Transition in the Wave of a Thin Flat Plate Placed Parallel to a Uniform Flow, J. of Fluid Mechanics, Sep. 1961, p. 321.

21. Goldstien: Modern Development in Fluid Dynamics - Wakes - Vol. II, p. 550.

22. Rouse: Engineering Hydraulics (Chapter I), 1950.

Nomenclature

R_e = Reynolds' number $(\frac{DV}{\nu})$.

D, d = diameter of circular cylinder (ft).

h = depth of flow (ft).

v, u = velocity of flow (fps).

ν = kinematic viscosity (ft^2/sec).

V_v = velocity of eddy behind cylinder.

S = Strauhal number (fD/v), vibration in lateral (y) direction only.

S_x = Strauhal number (f_xD/v), in longitudinal direction, both x, y vibrating.

S_y = Strauhal number (f_yD/v), in lateral direction, both x, y vibrating.

f = frequency of forced vibration in lateral direction only.

f_x = frequency of forced vibration in longitudinal direction, both x, y vibrating.

f_y = frequency of forced vibration in lateral direction, both x, y vibrating.

f_s = frequency of forced vibration in lateral direction for stationary cylinder.

f_n = natural frequency of the system, lateral direction.

f'_n = natural frequency of the system, longitudinal direction.

δ_x = amplitude in lateral direction (from wave crest to trough).

δ_y = amplitude in longitudinal direction (from wave crest to trough).

P = force.

P_x = max. hydro-elastic vibrating force in longitudinal direction.

P_y = max. hydro-elastic vibrating force in lateral direction.

$B_{\Delta px}$ = response coe. of vibrating drag, $\Delta P_x / \rho \frac{U^2}{2} A$.

B_{py} = response coe. of vibrating lift, $P_y / \rho \frac{U^2}{2} A$.

V_{res} = velocity of resonance, lateral vibration only.

V'_{res} = velocity of resonance, longitudinal vibration only.

R_{res} = Reynolds' number, when only lateral resonance occurs.

R'_{res} = Reynolds' number, when only longitudinal resonance occurs.

X, Y = fluid force acting on cylinder in x, y direction.

U = velocity of uniform flow.

w = complex function.

z = complex variable.

Γ = circulation.

Δp = pressure difference.

v = local velocity in the flow.

ρ = mass density.

t = time.

M = mass of the system.

k = spring constant.

E = modulus of elasticity.

I = moment of inertia.

L = length of beam.

T = period.

p = $\frac{k}{M}$, circular frequency.

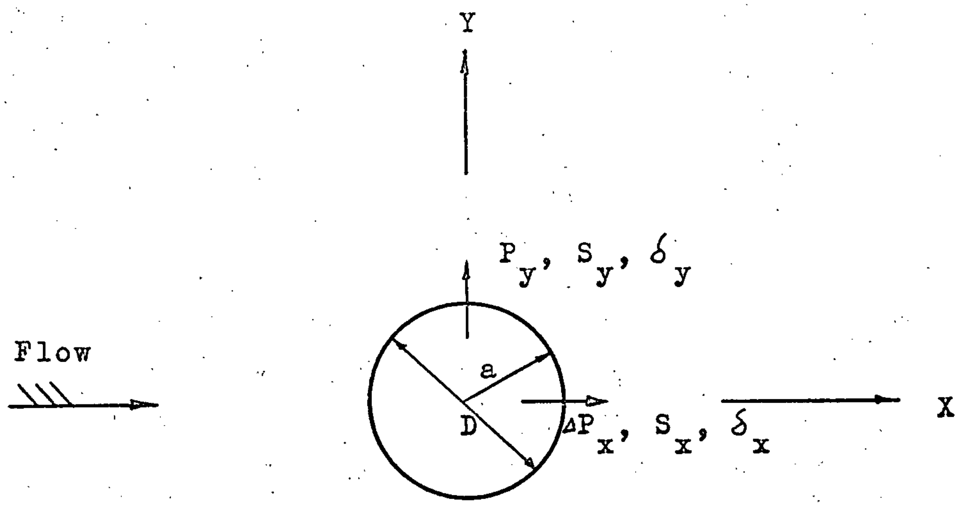

Fig. 9 Definition sketch

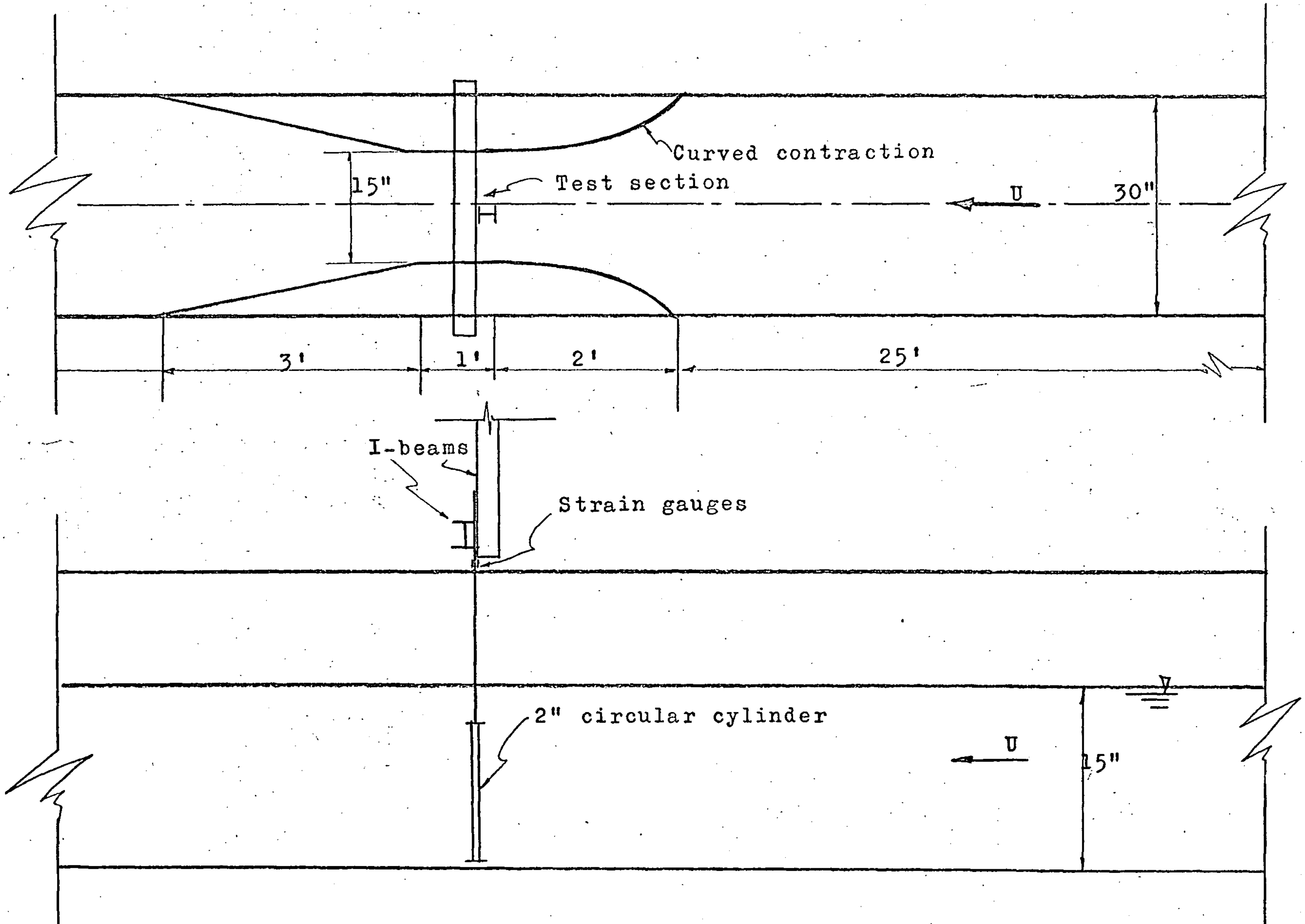

Fig. 10 Water flume

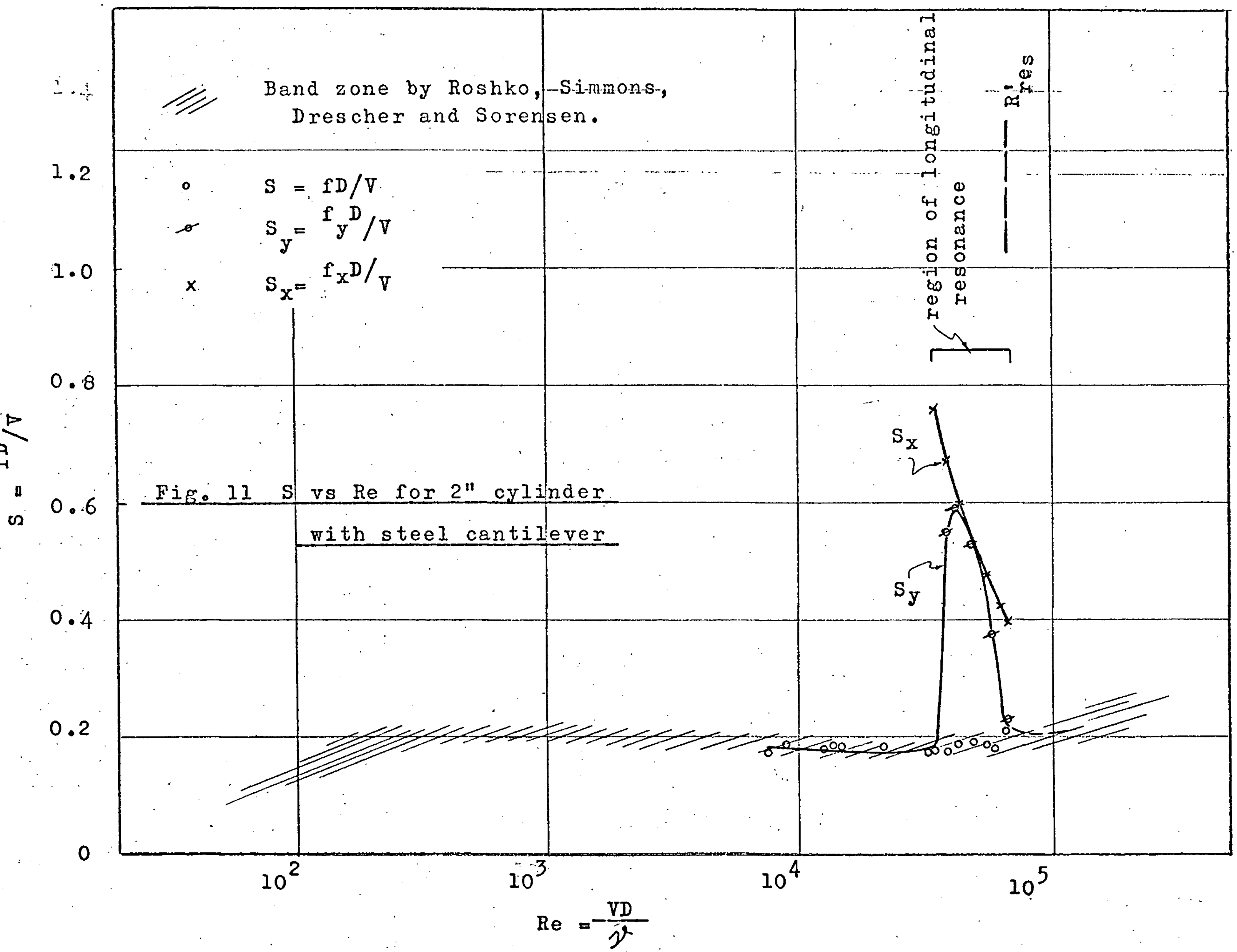

Fig. 11 S vs Re for 2" cylinder with steel cantilever

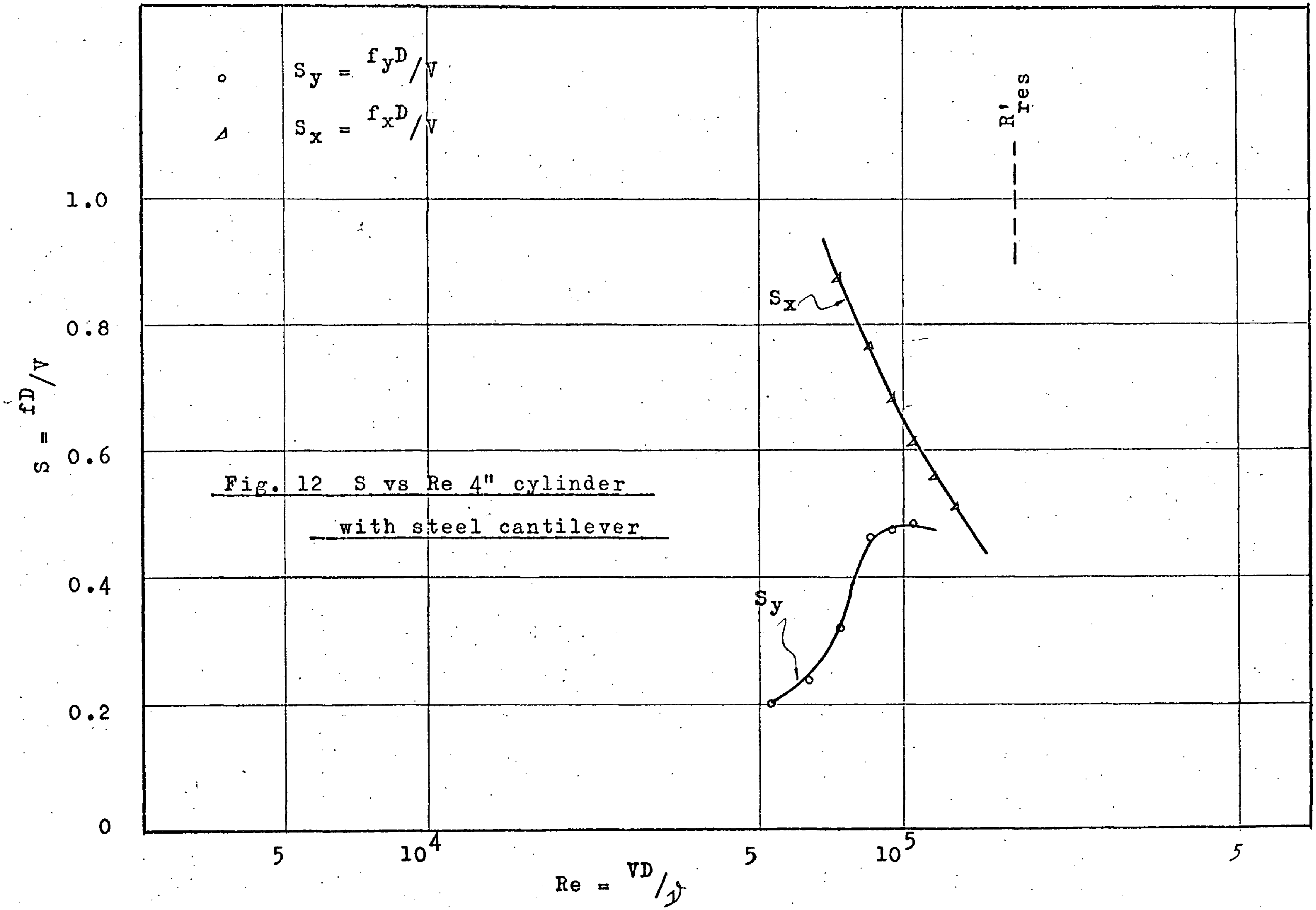

Fig. 12 S vs Re 4" cylinder with steel cantilever

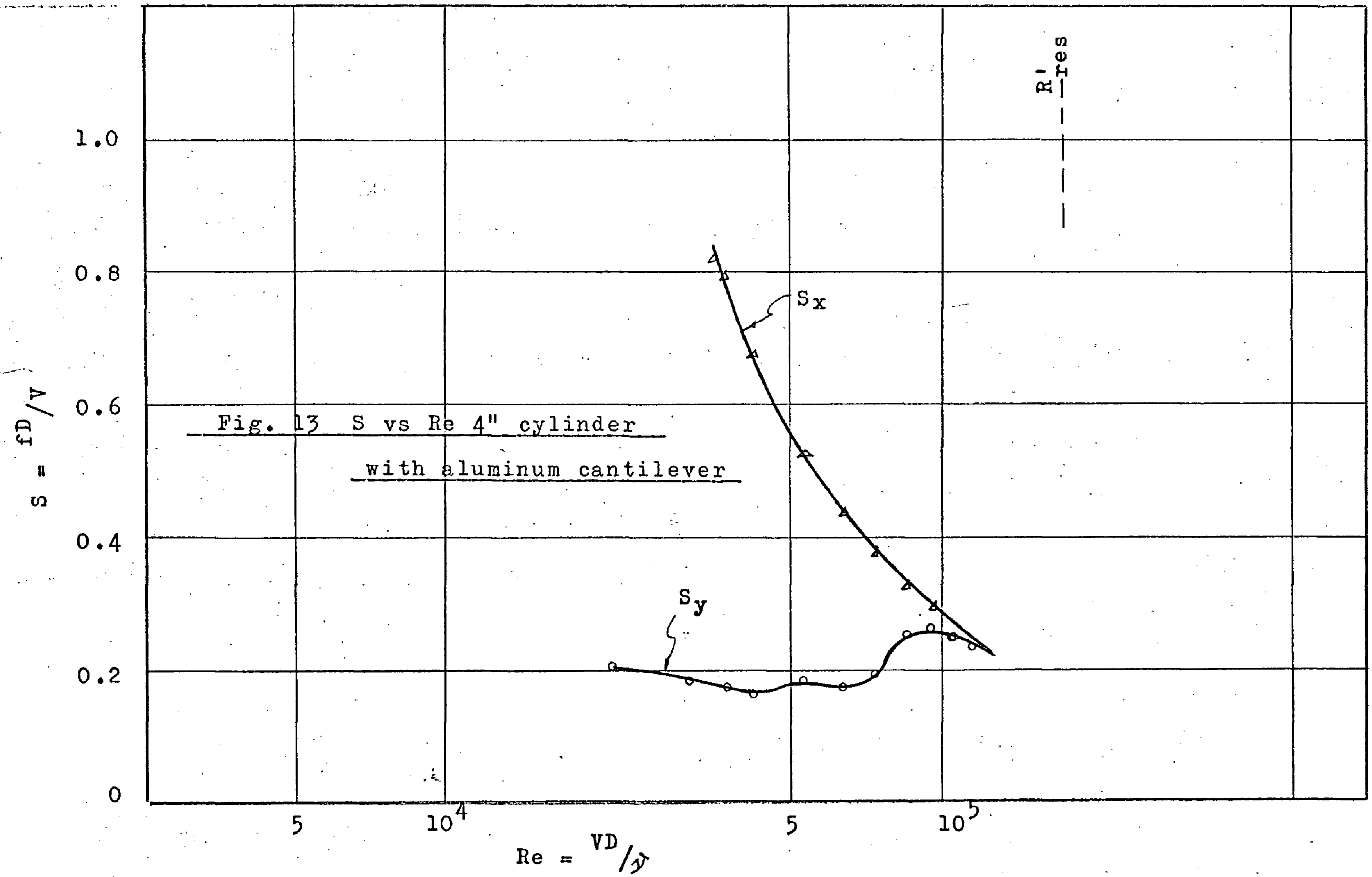

Fig. 13 S vs Re 4" cylinder with aluminum cantilever

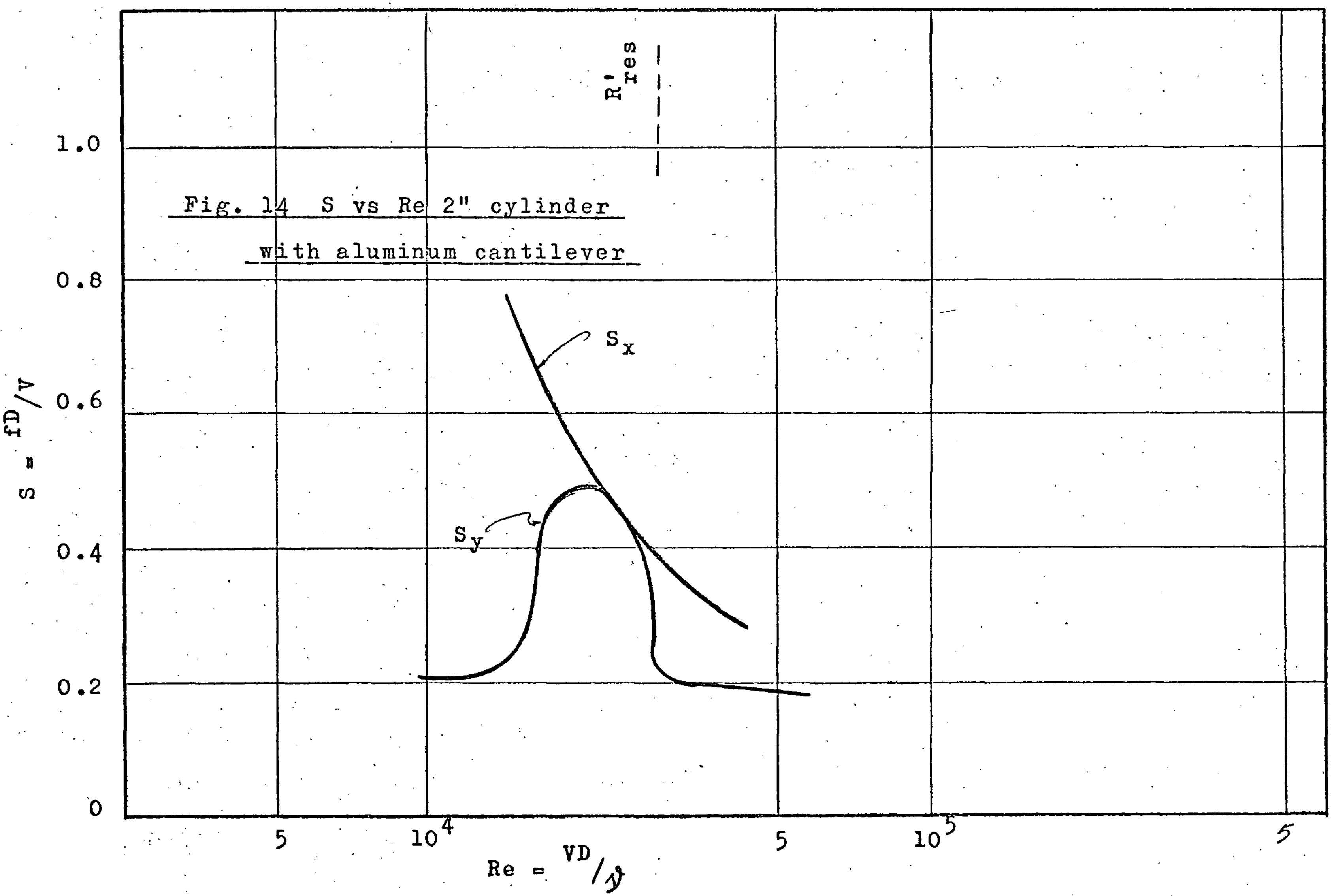

Fig. 14 S vs Re 2" cylinder with aluminum cantilever

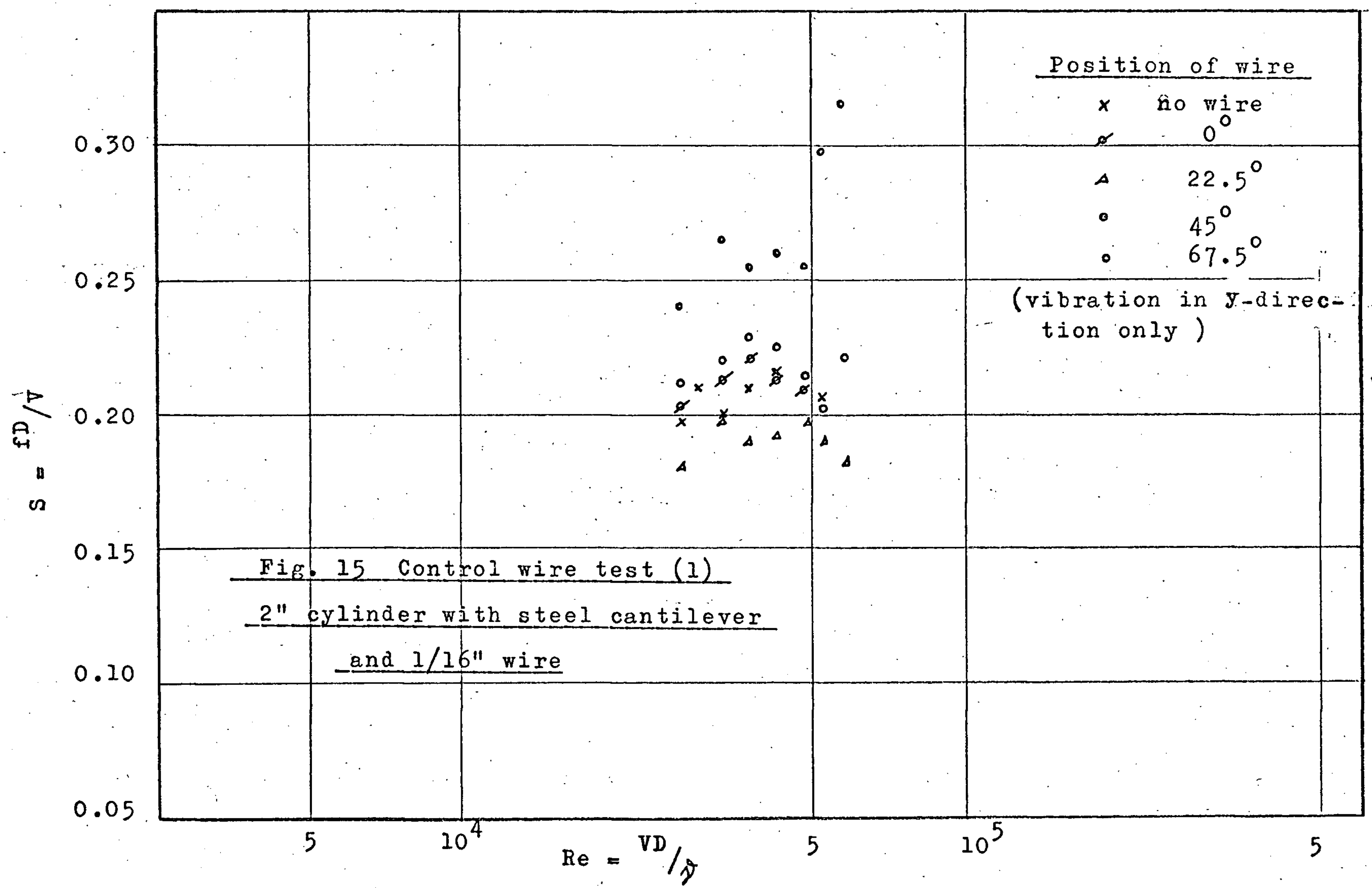

Fig. 15 Control wire test (1)
2" cylinder with steel cantilever
and 1/16" wire

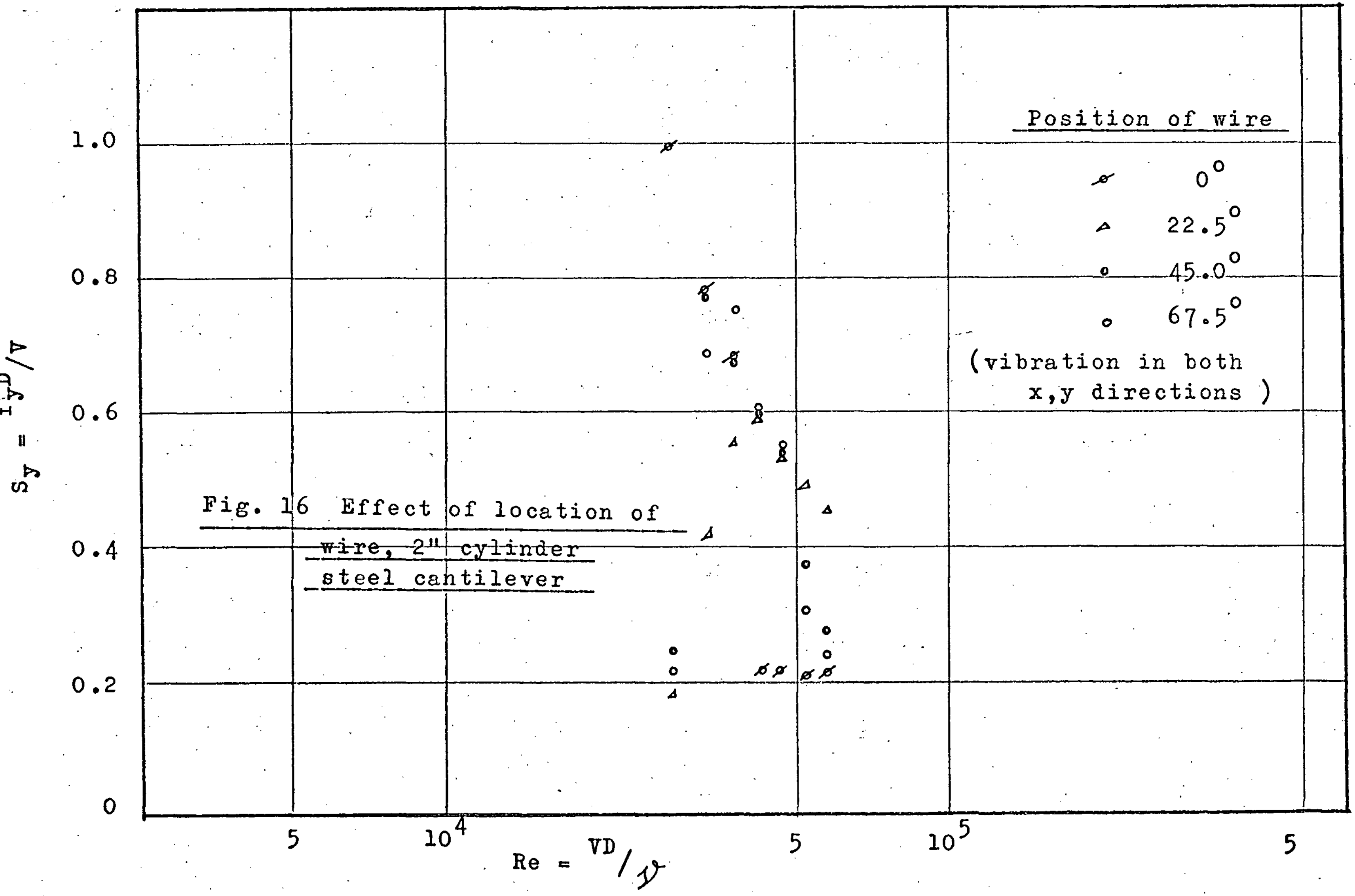

Fig. 16 Effect of location of wire, 2" cylinder steel cantilever

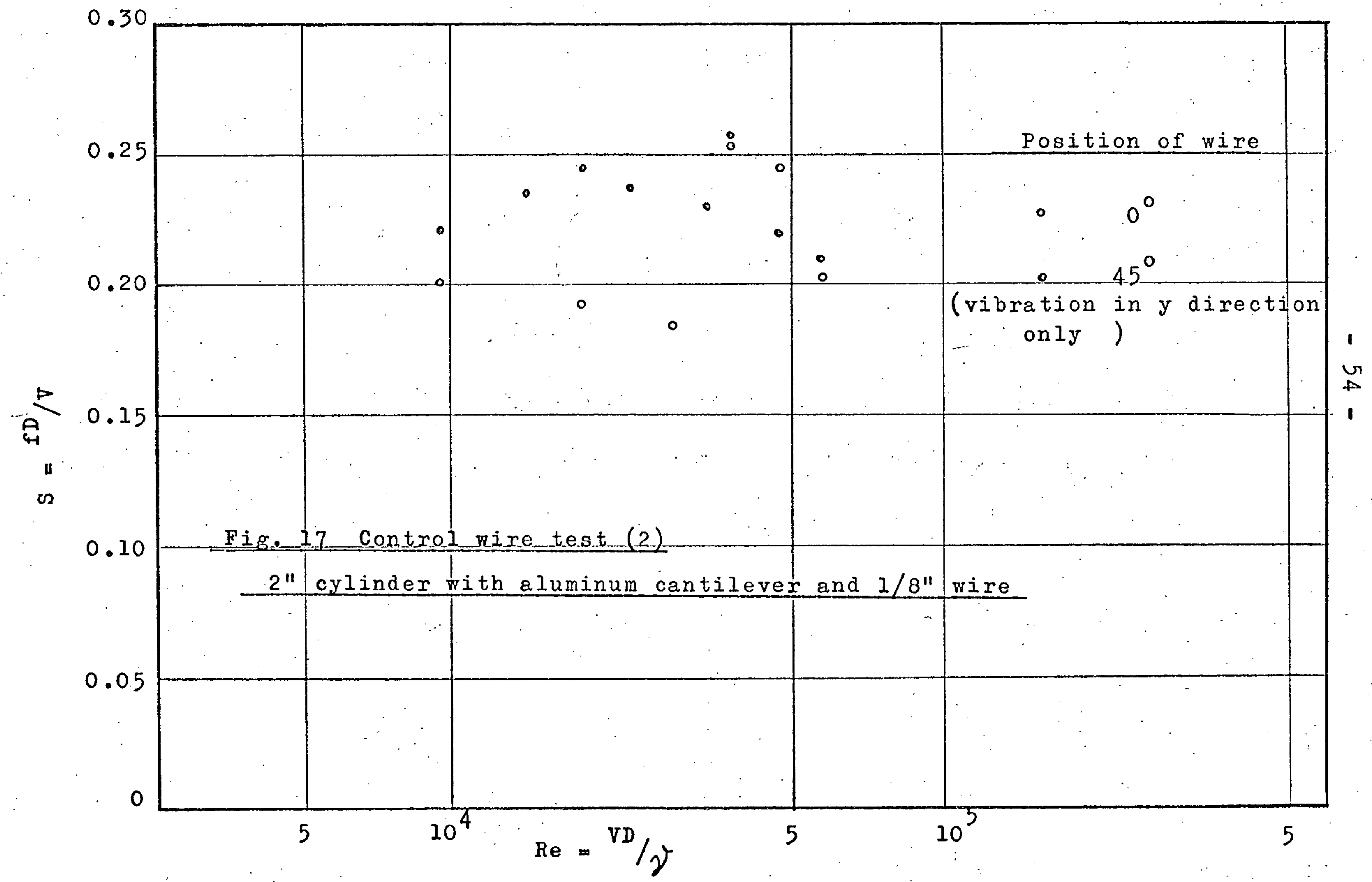

Fig. 17 Control wire test (2)

2" cylinder with aluminum cantilever and 1/8" wire

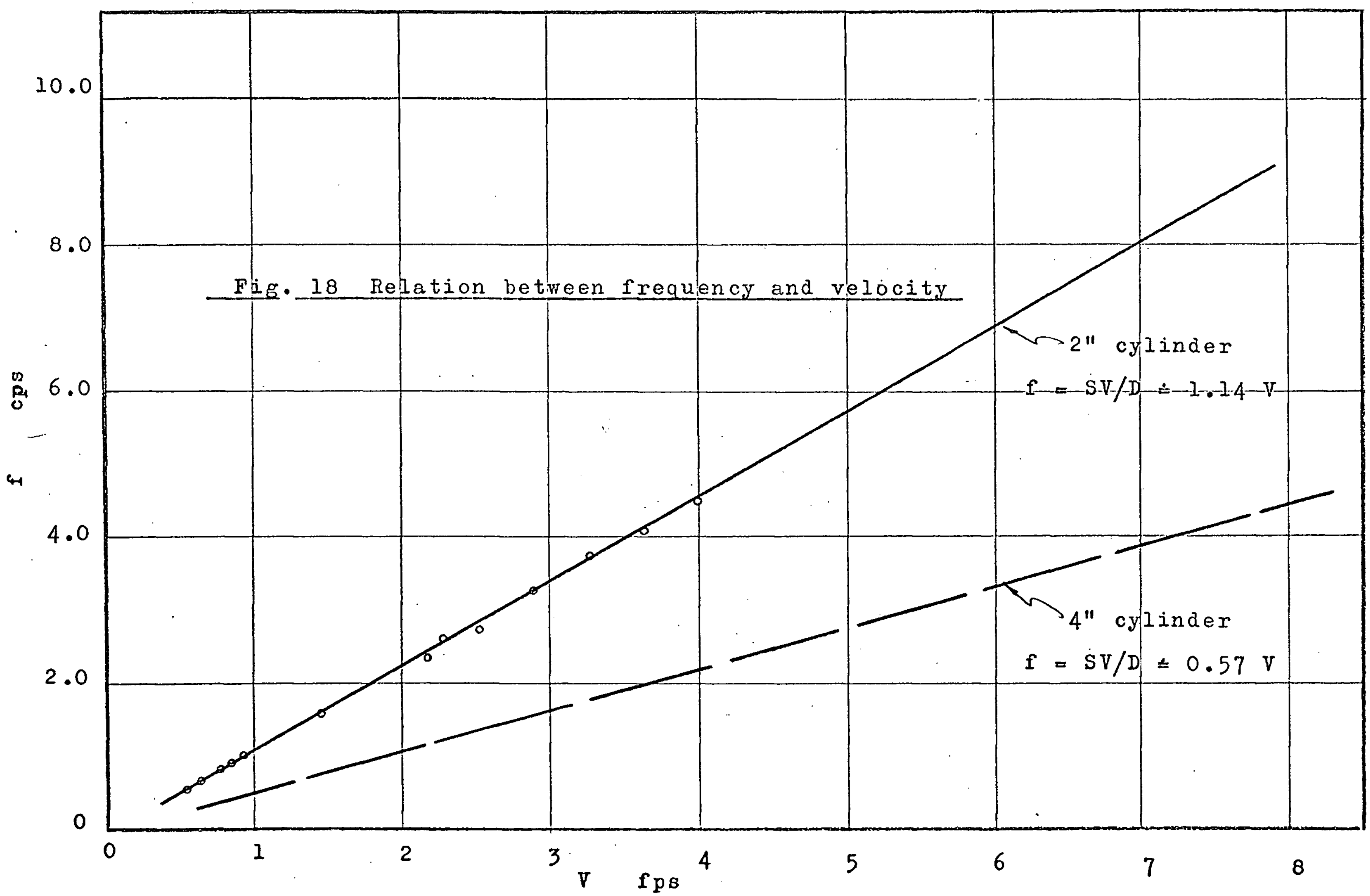

Fig. 18 Relation between frequency and velocity
2" cylinder
f = SV/D ≐ 1.14 V
4" cylinder
f = SV/D ≐ 0.57 V
f cps
V fps
10.0
8.0
6.0
4.0
2.0
0
0
1
2
3
4
5
6
7
8

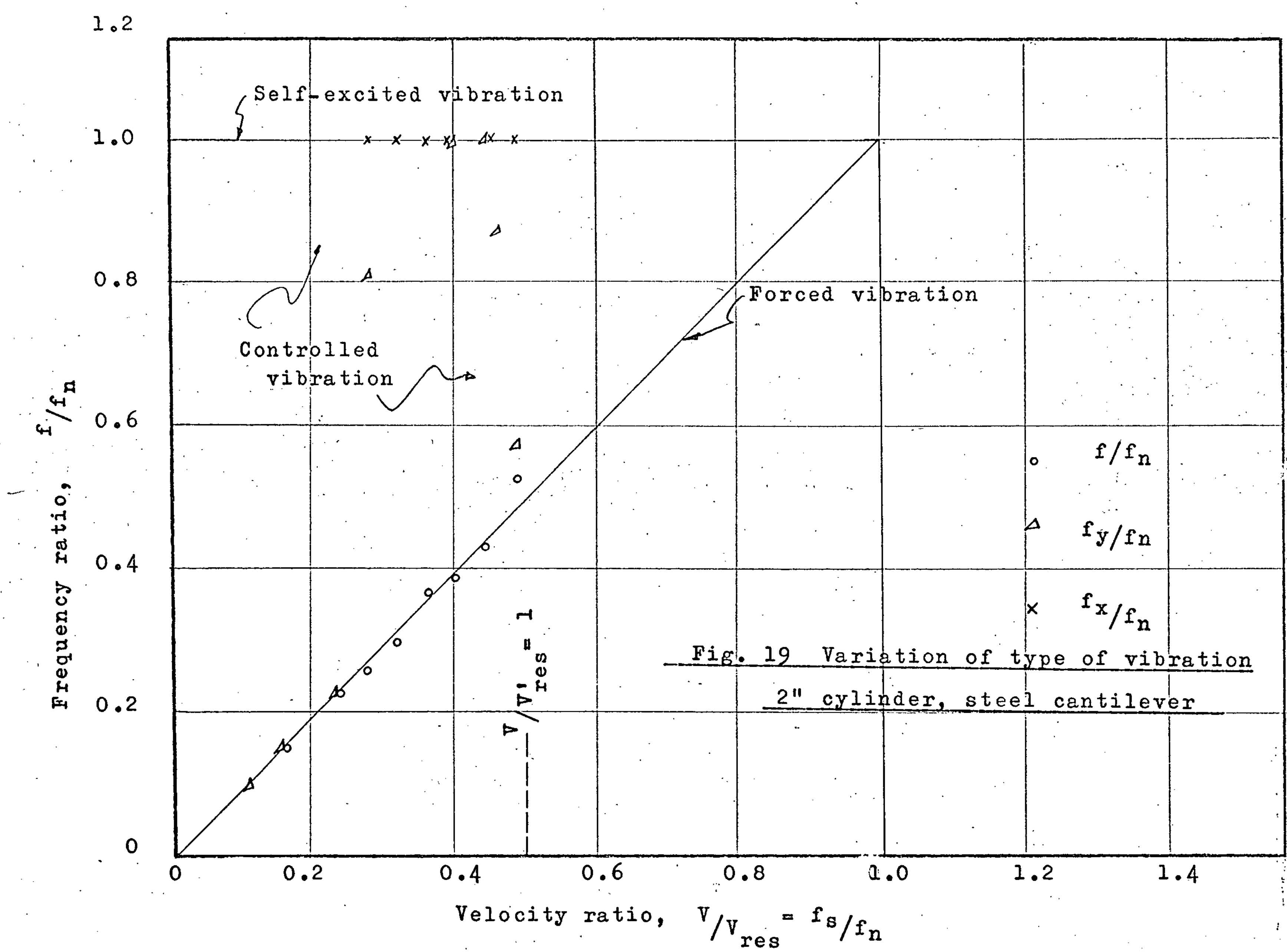

Fig. 19 Variation of type of vibration

2" cylinder, steel cantilever

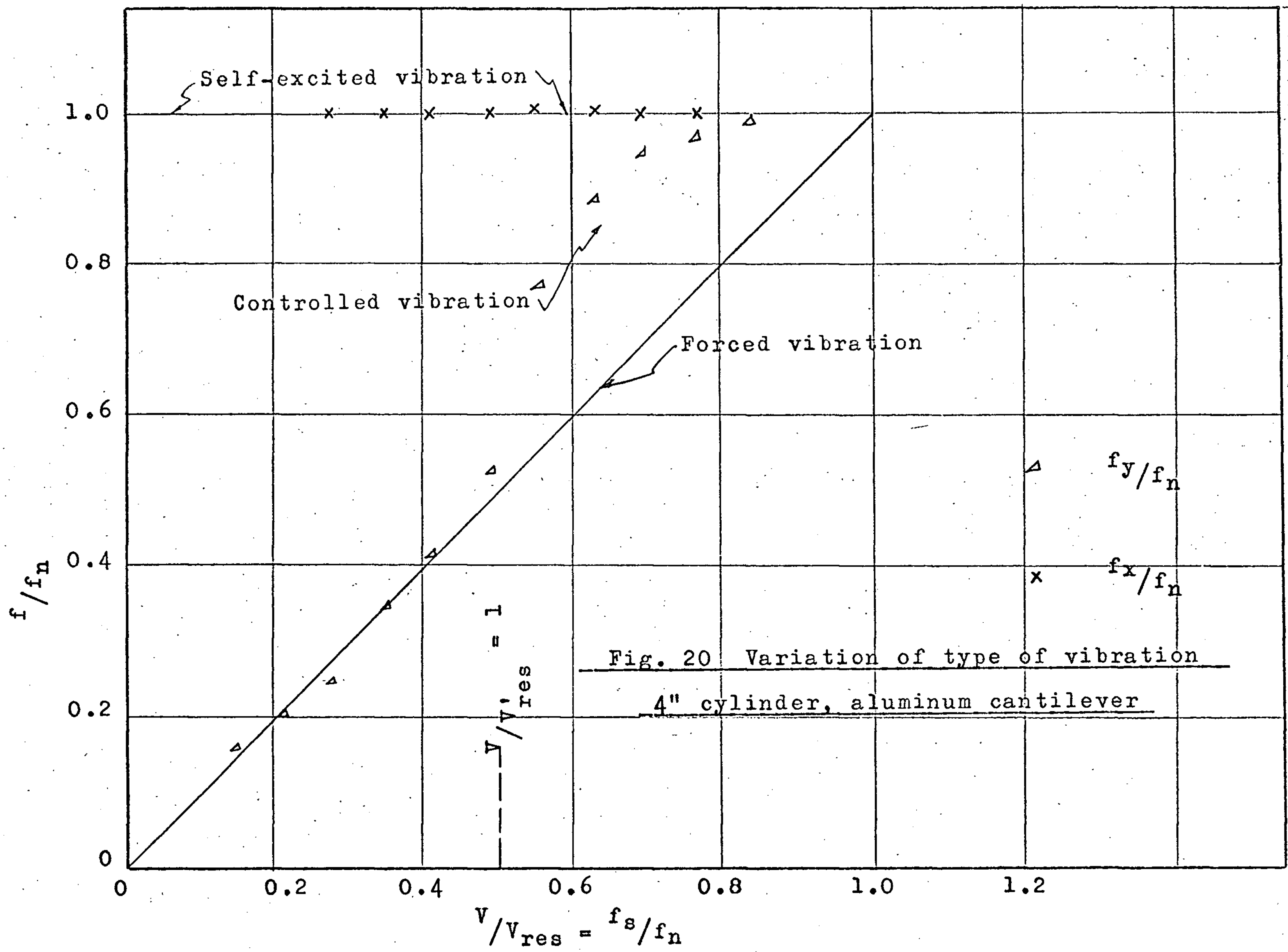

Fig. 20 Variation of type of vibration
4" cylinder, aluminum cantilever

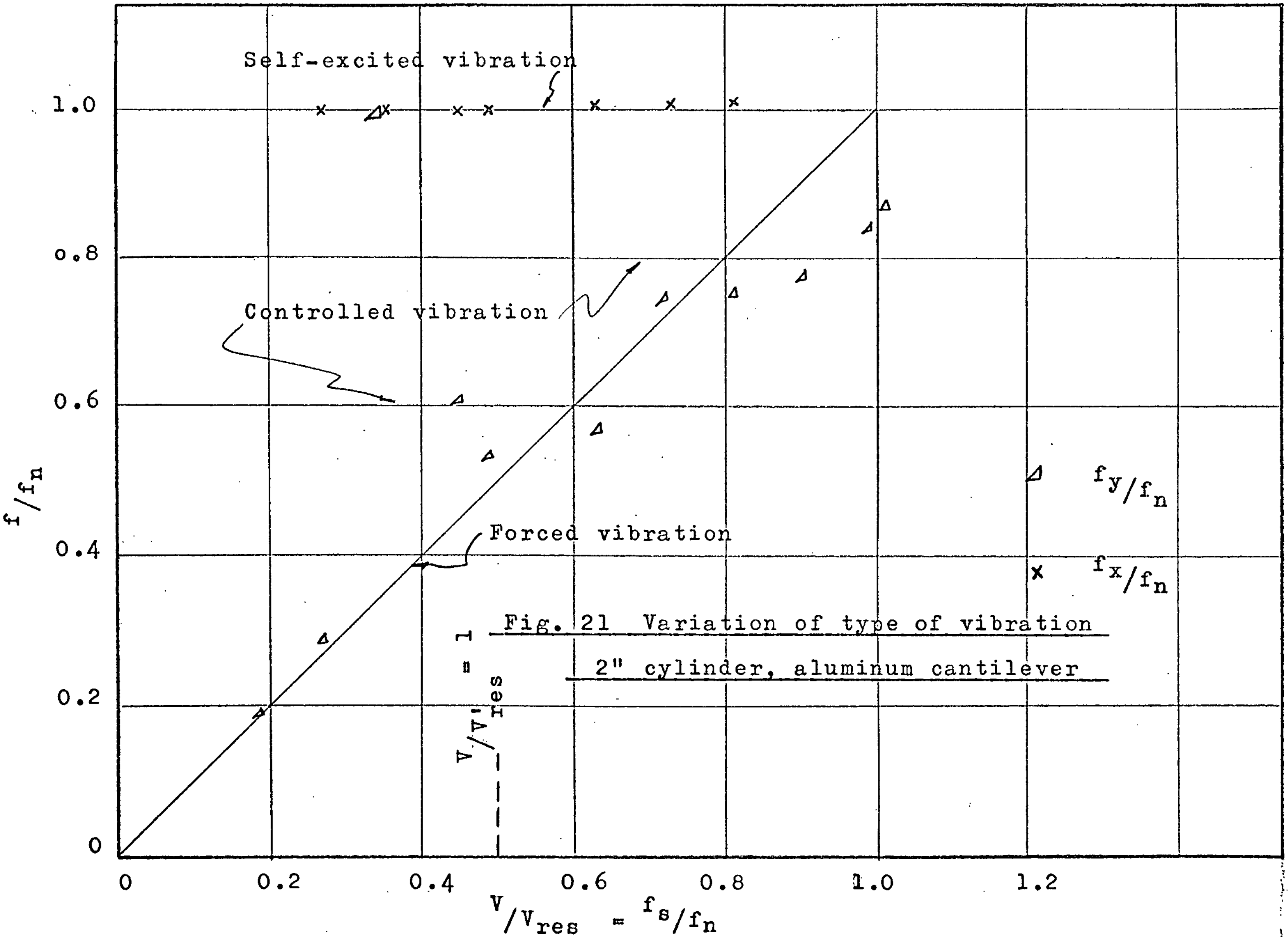

Fig. 21 Variation of type of vibration

2" cylinder, aluminum cantilever

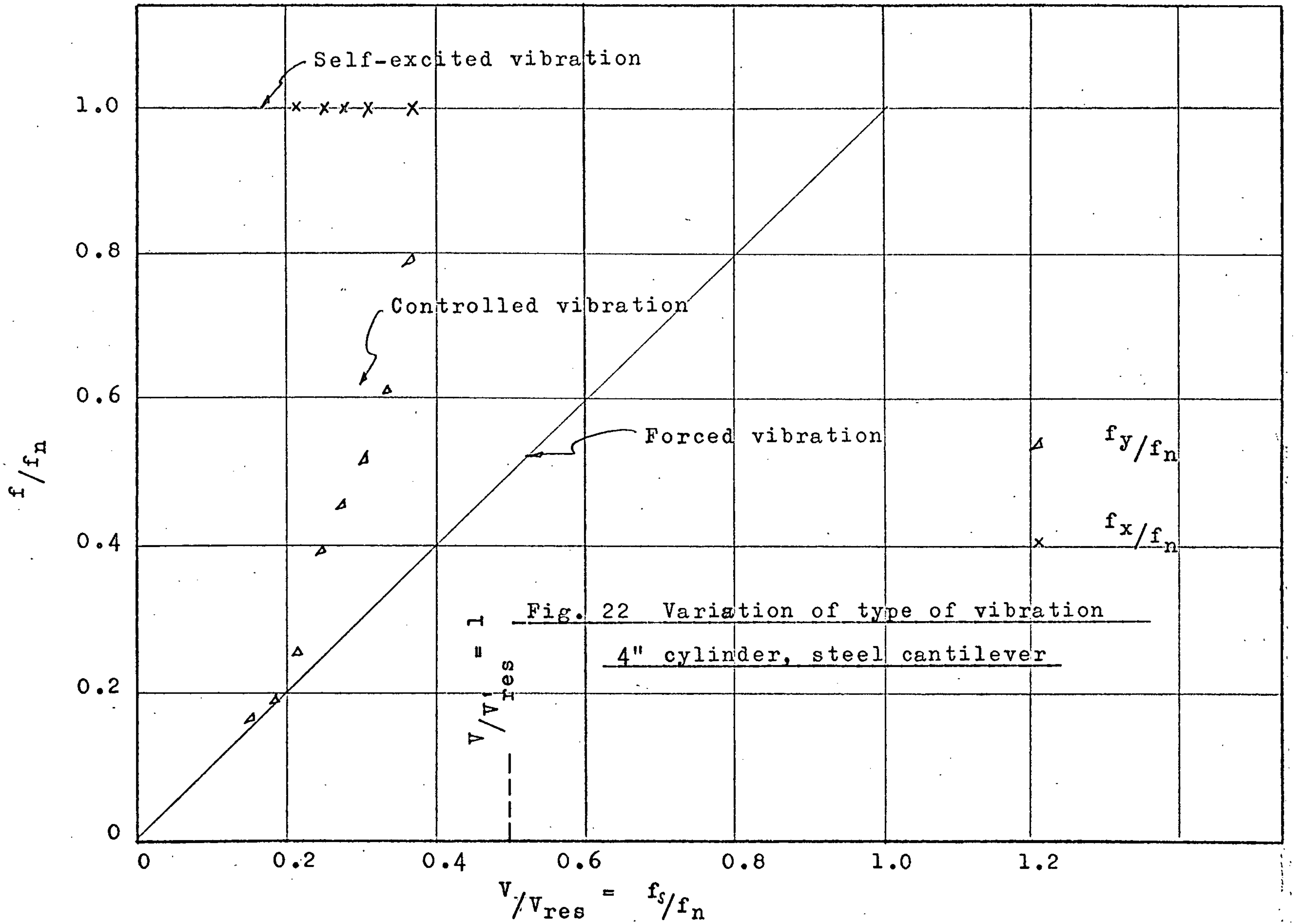

Fig. 22 Variation of type of vibration

4" cylinder, steel cantilever

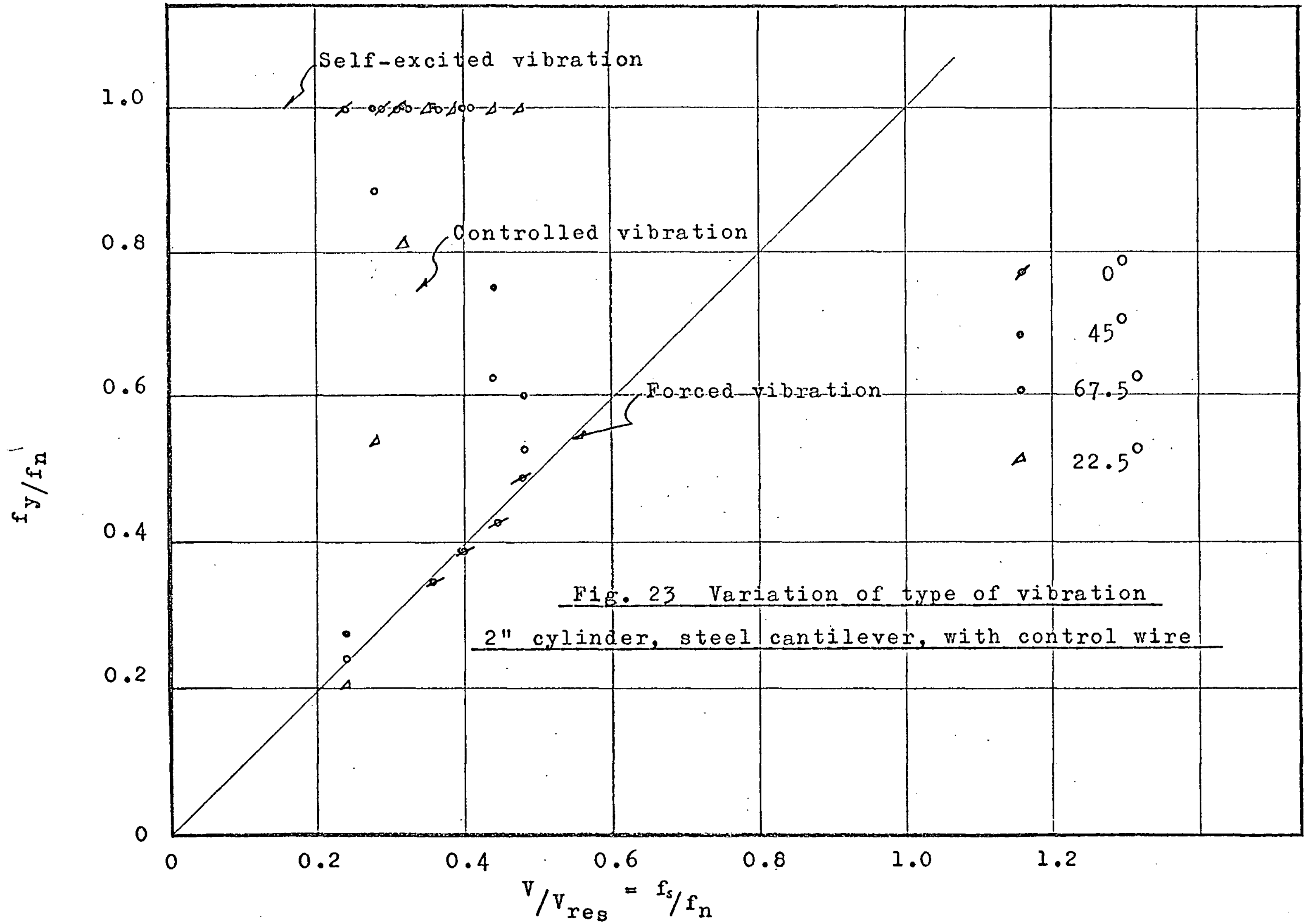

Fig. 23 Variation of type of vibration

2" cylinder, steel cantilever, with control wire

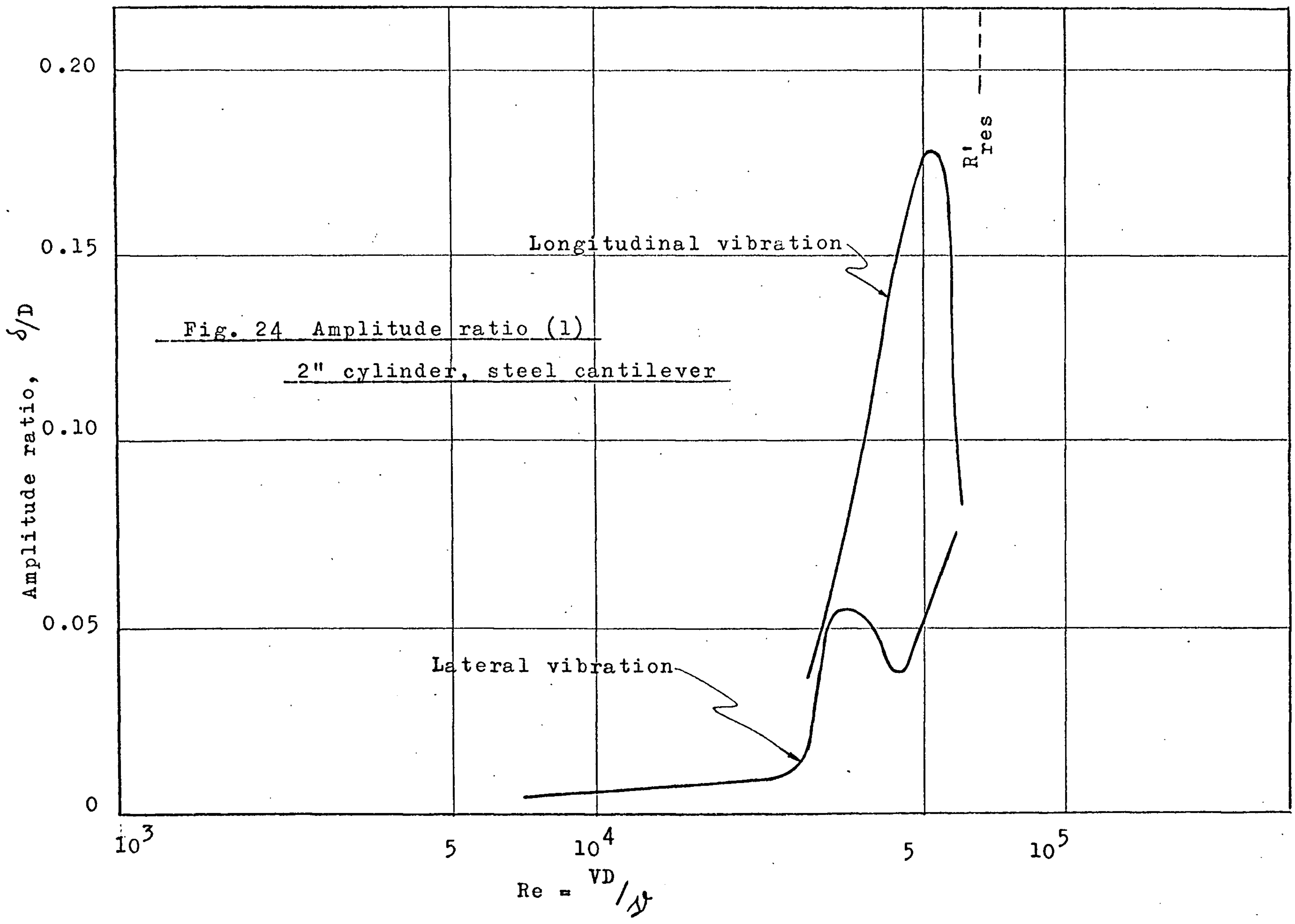

Fig. 24 Amplitude ratio (1)
2" cylinder, steel cantilever

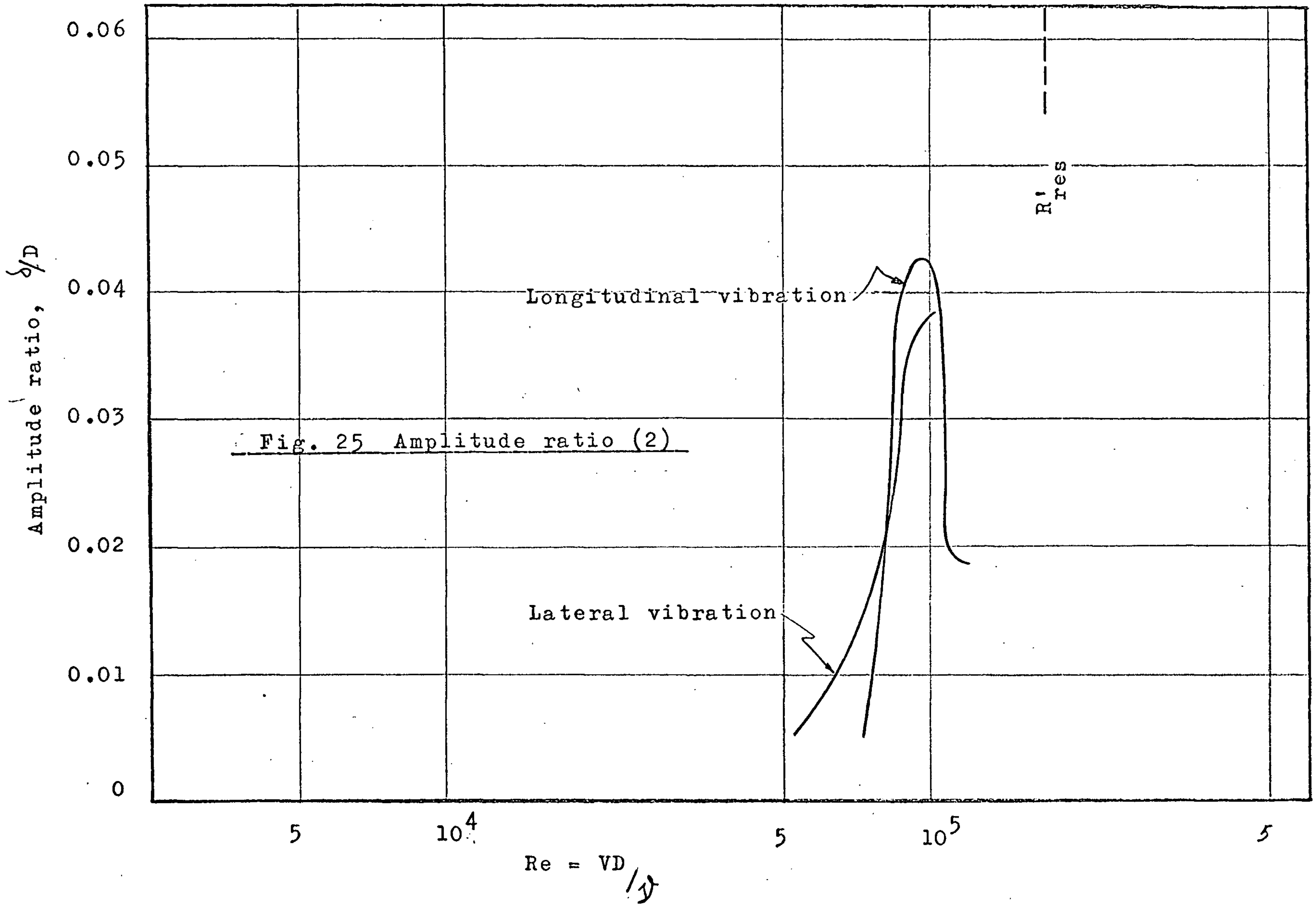

Fig. 25 Amplitude ratio (2)

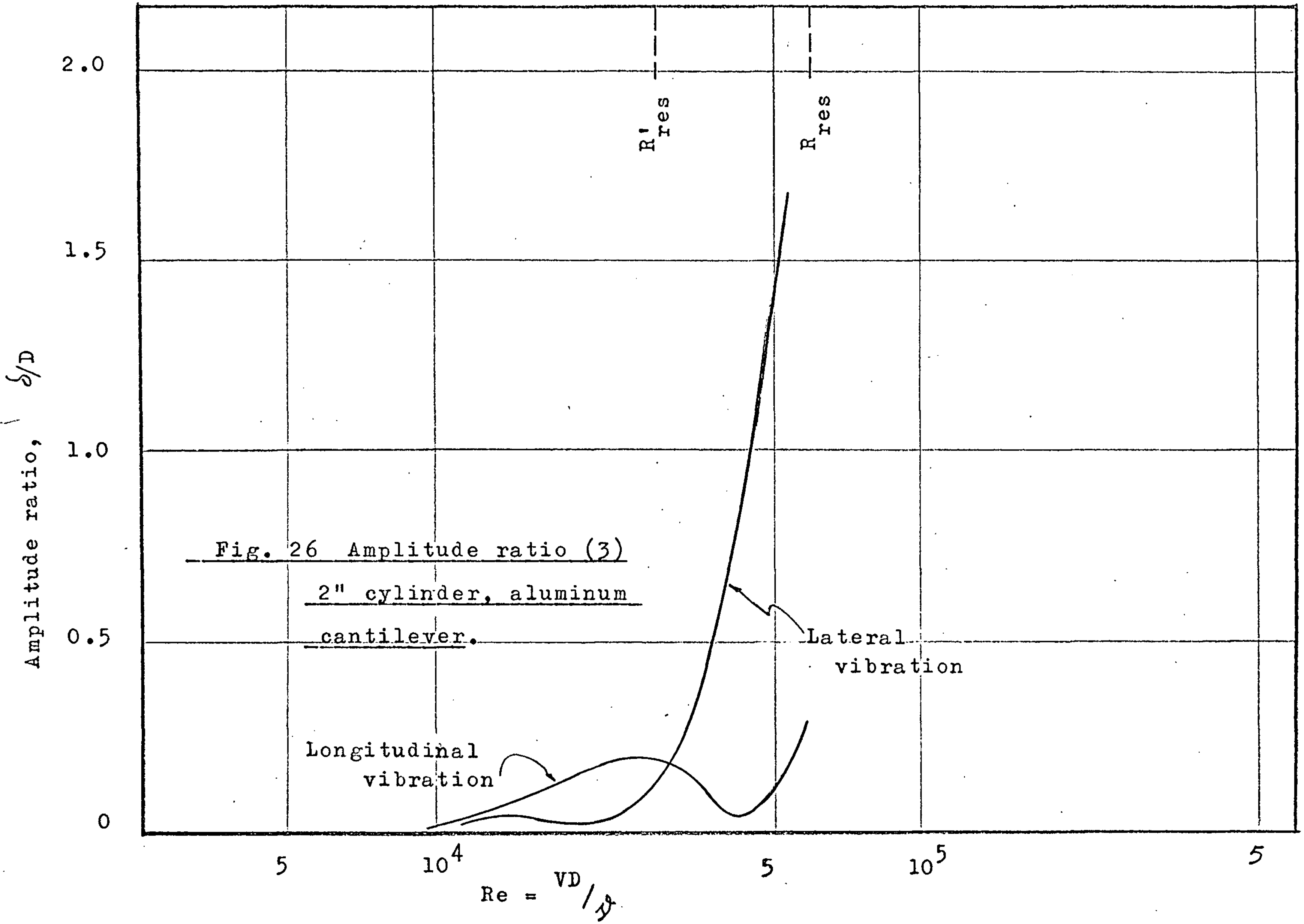

<u>Fig. 26 Amplitude ratio (3)</u>
<u>2" cylinder, aluminum</u>
<u>cantilever.</u>

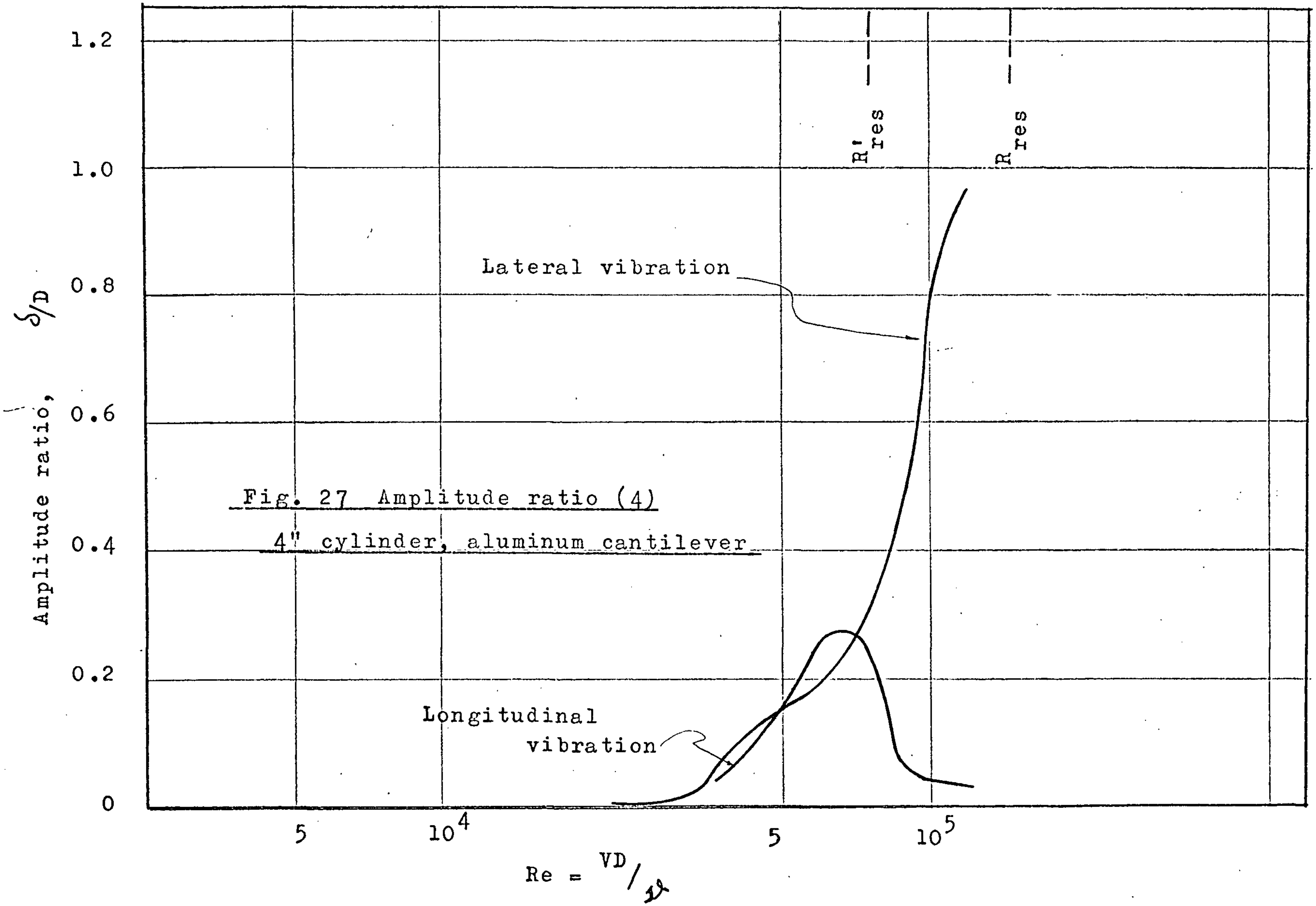

Fig. 27 Amplitude ratio (4)
4" cylinder, aluminum cantilever

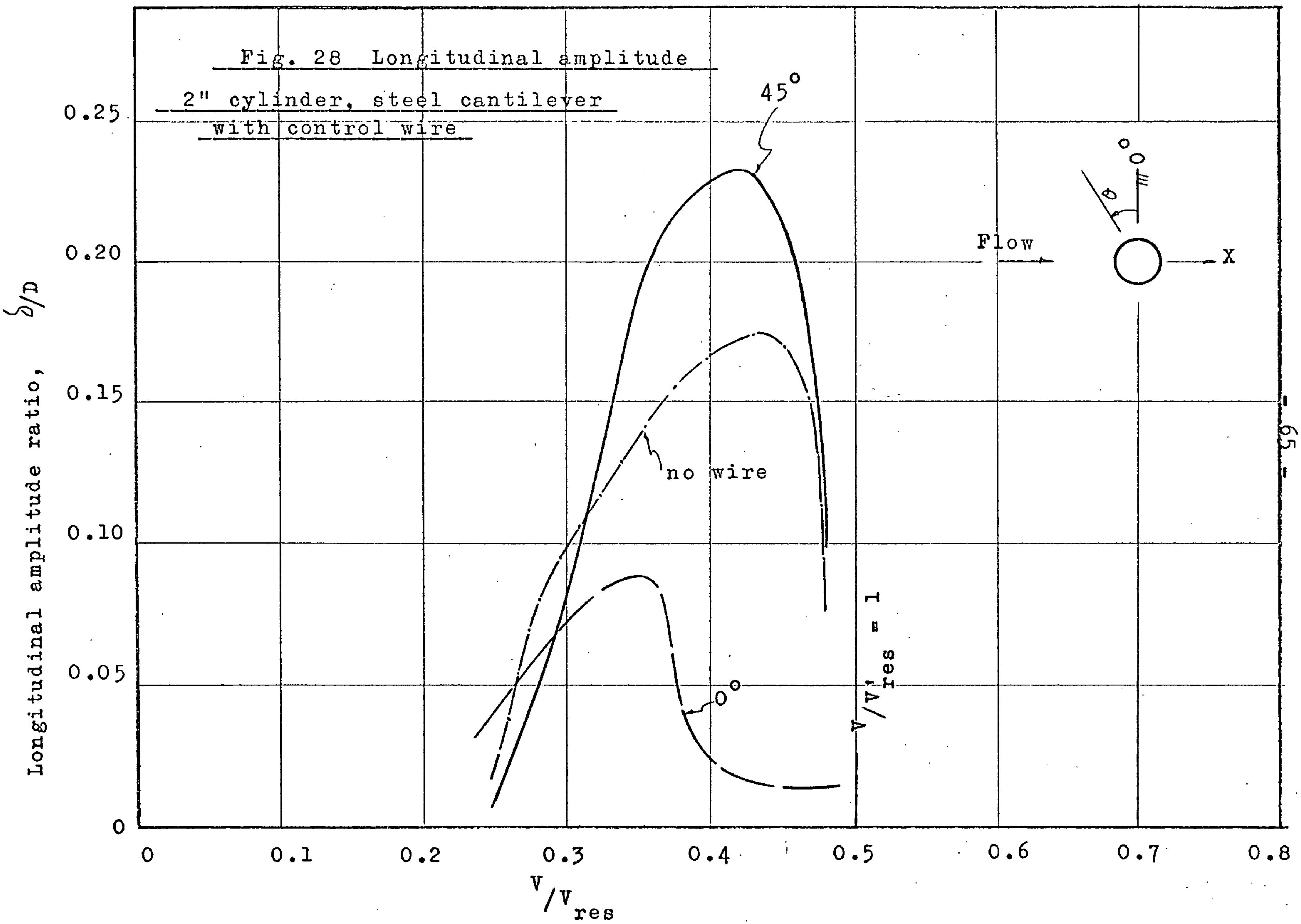

Fig. 28 Longitudinal amplitude
2" cylinder, steel cantilever
with control wire

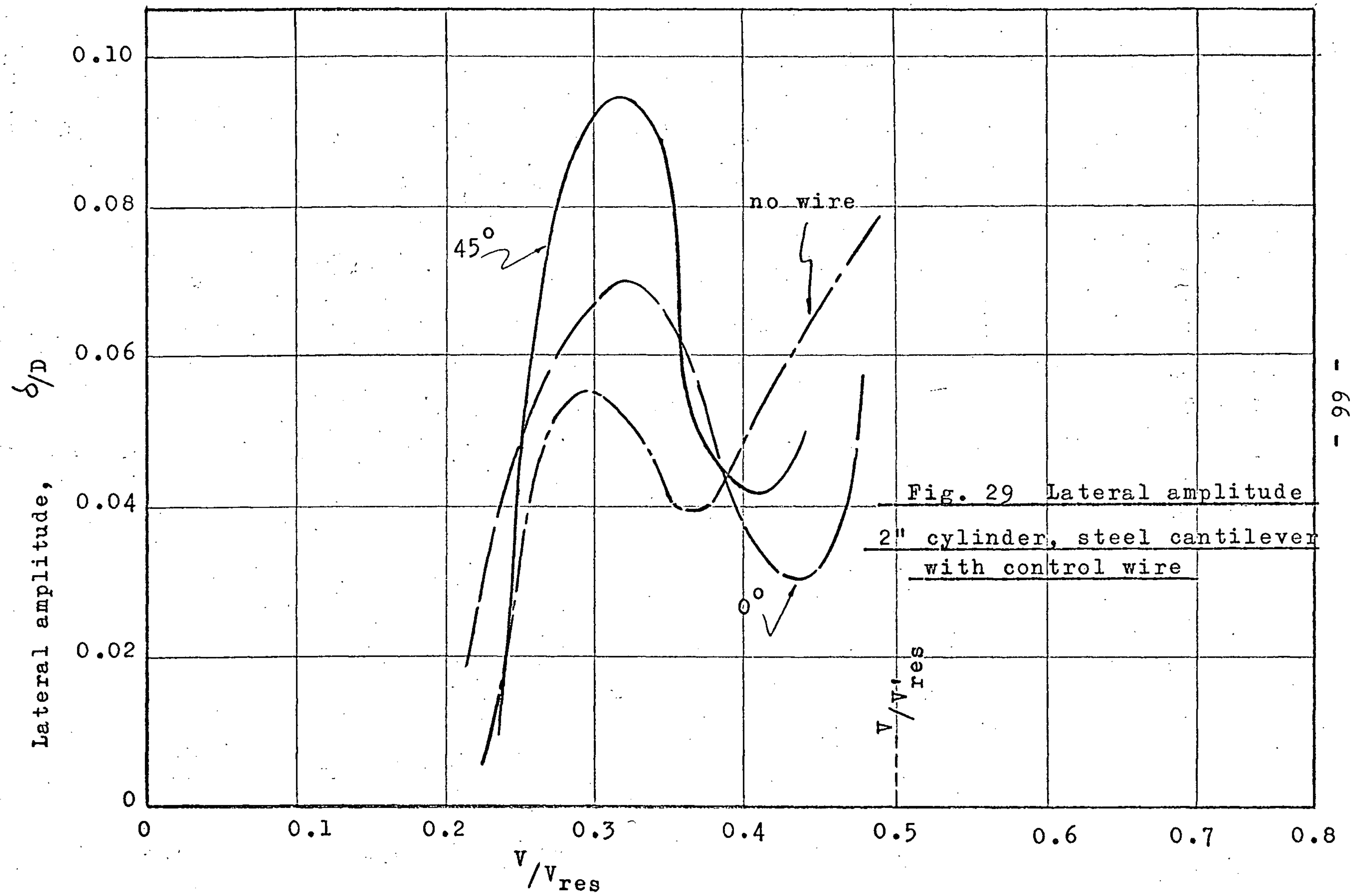

Fig. 29 Lateral amplitude
2" cylinder, steel cantilever
with control wire

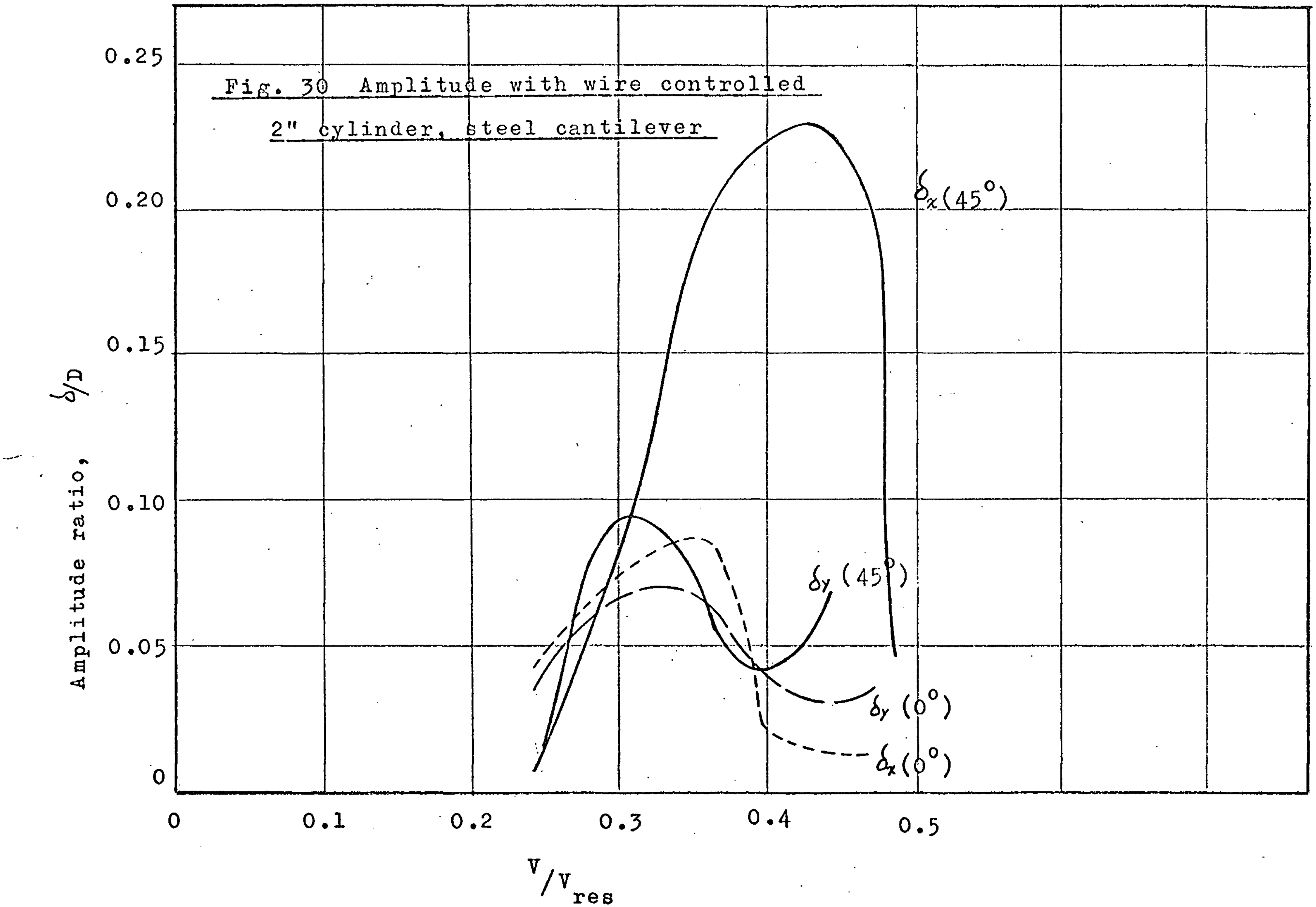

Fig. 30 Amplitude with wire controlled
2" cylinder, steel cantilever
0.25
0.20
0.15
0.10
0.05
0
Amplitude ratio, δ/D
0
0.1
0.2
0.3
0.4
0.5
V/V res
δx(45°)
δy (45°)
δy (0°)
δx(0°)

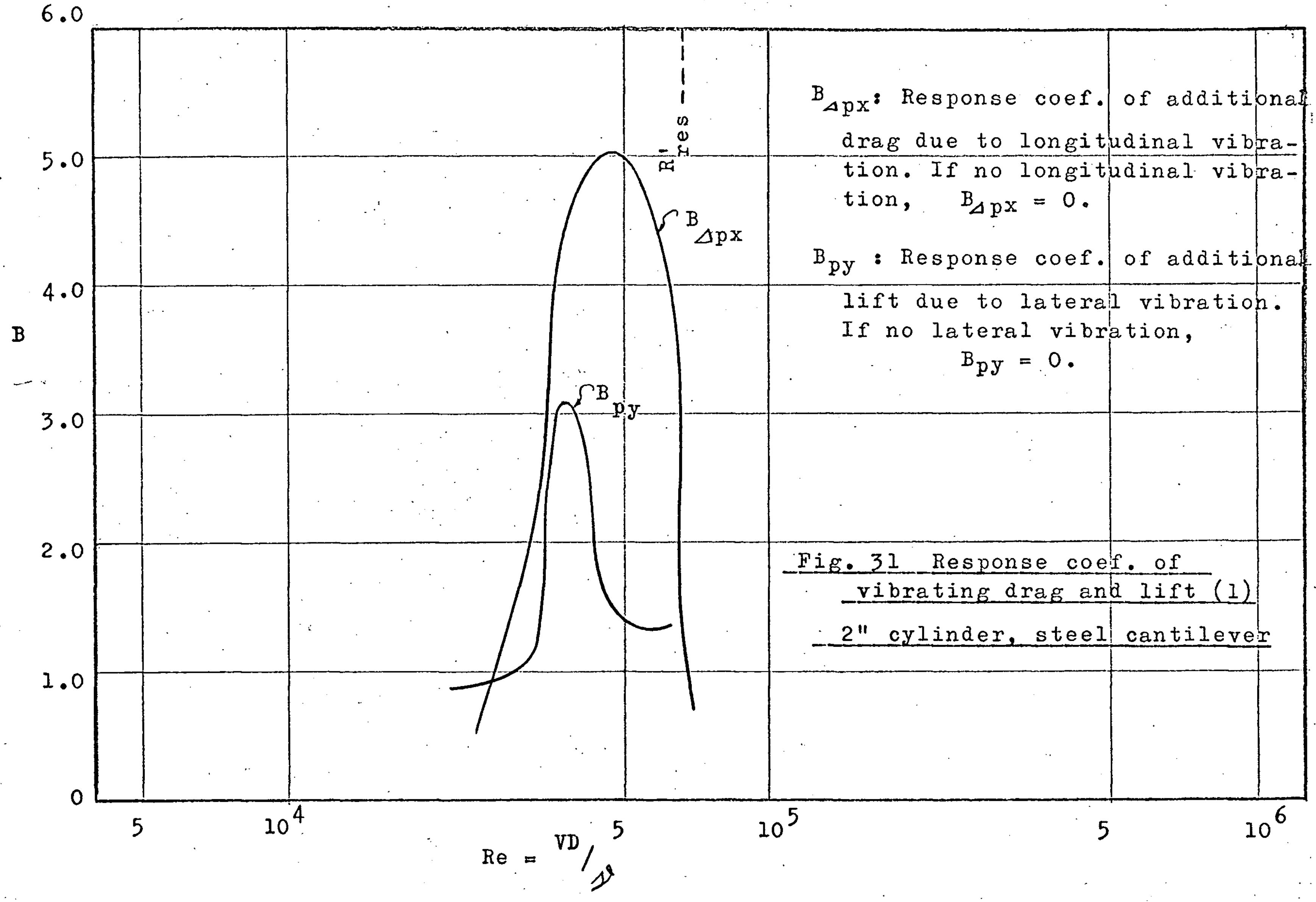

Fig. 31 Response coef. of vibrating drag and lift (1)
2" cylinder, steel cantilever

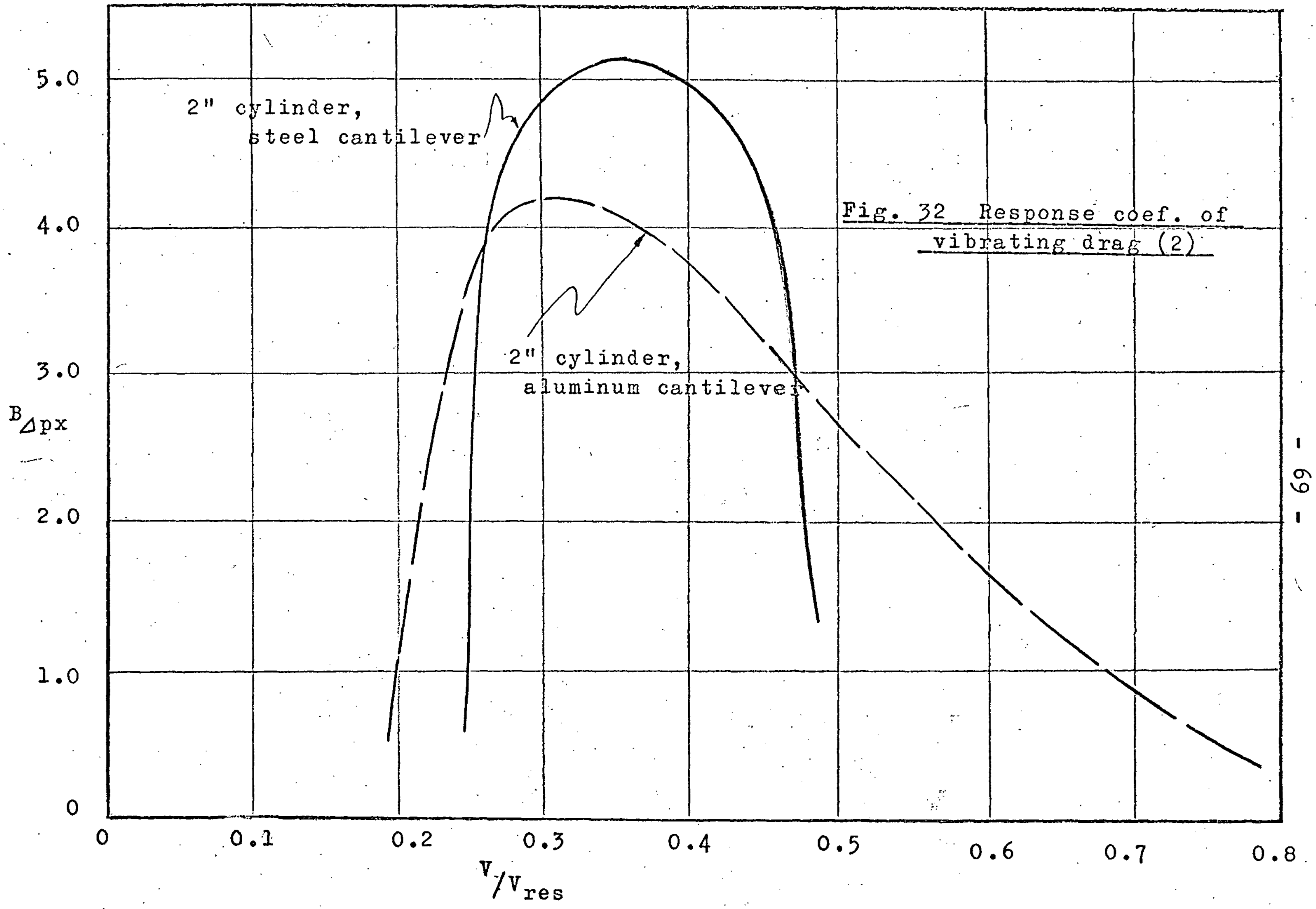

Fig. 32 Response coef. of vibrating drag (2)

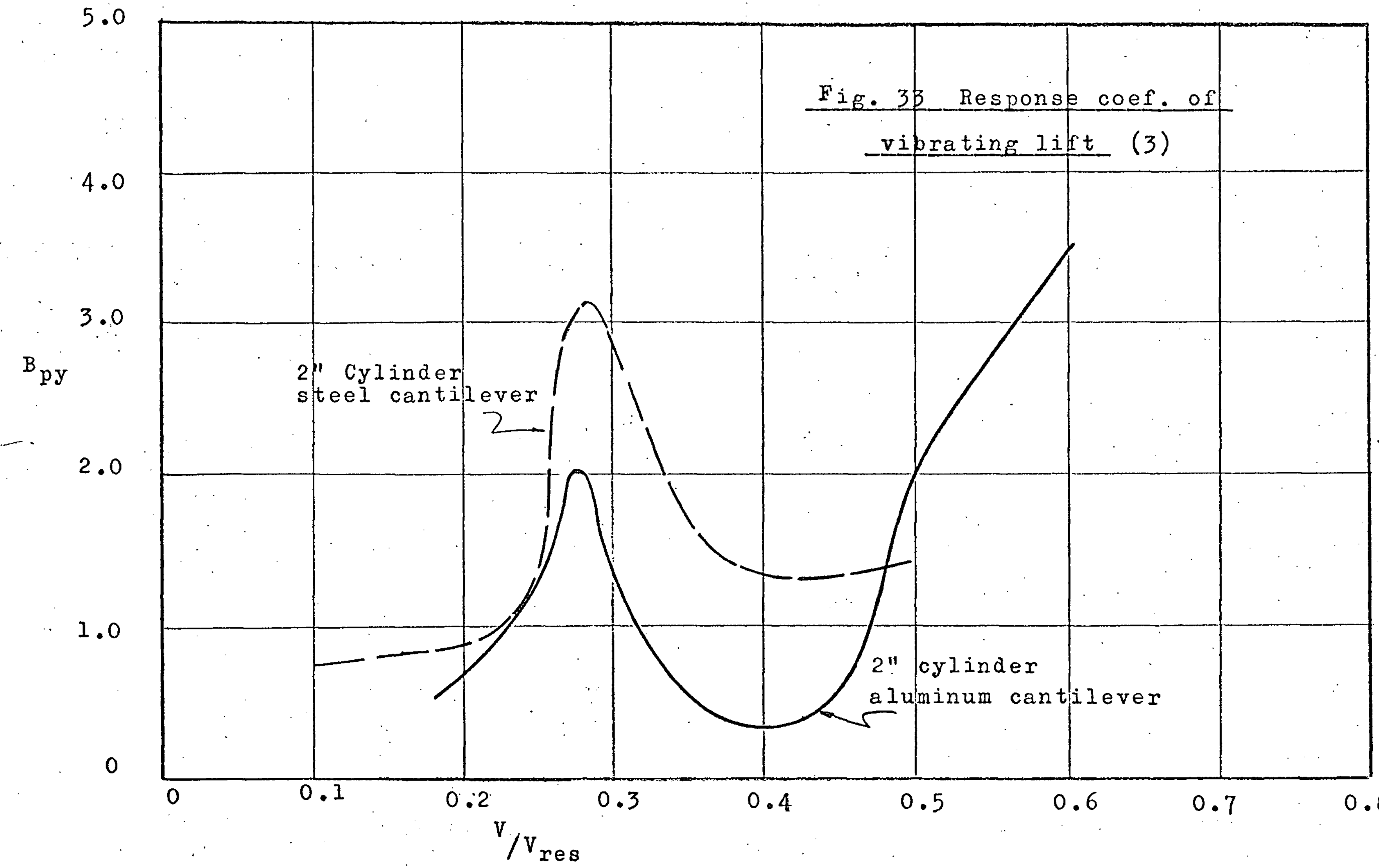

Fig. 33 Response coef. of vibrating lift (3)
5.0
4.0
3.0
2.0
1.0
0
B_{py}
2" Cylinder steel cantilever
2" cylinder aluminum cantilever
0
0.1
0.2
0.3
0.4
0.5
0.6
0.7
0.8
V/V_{res}

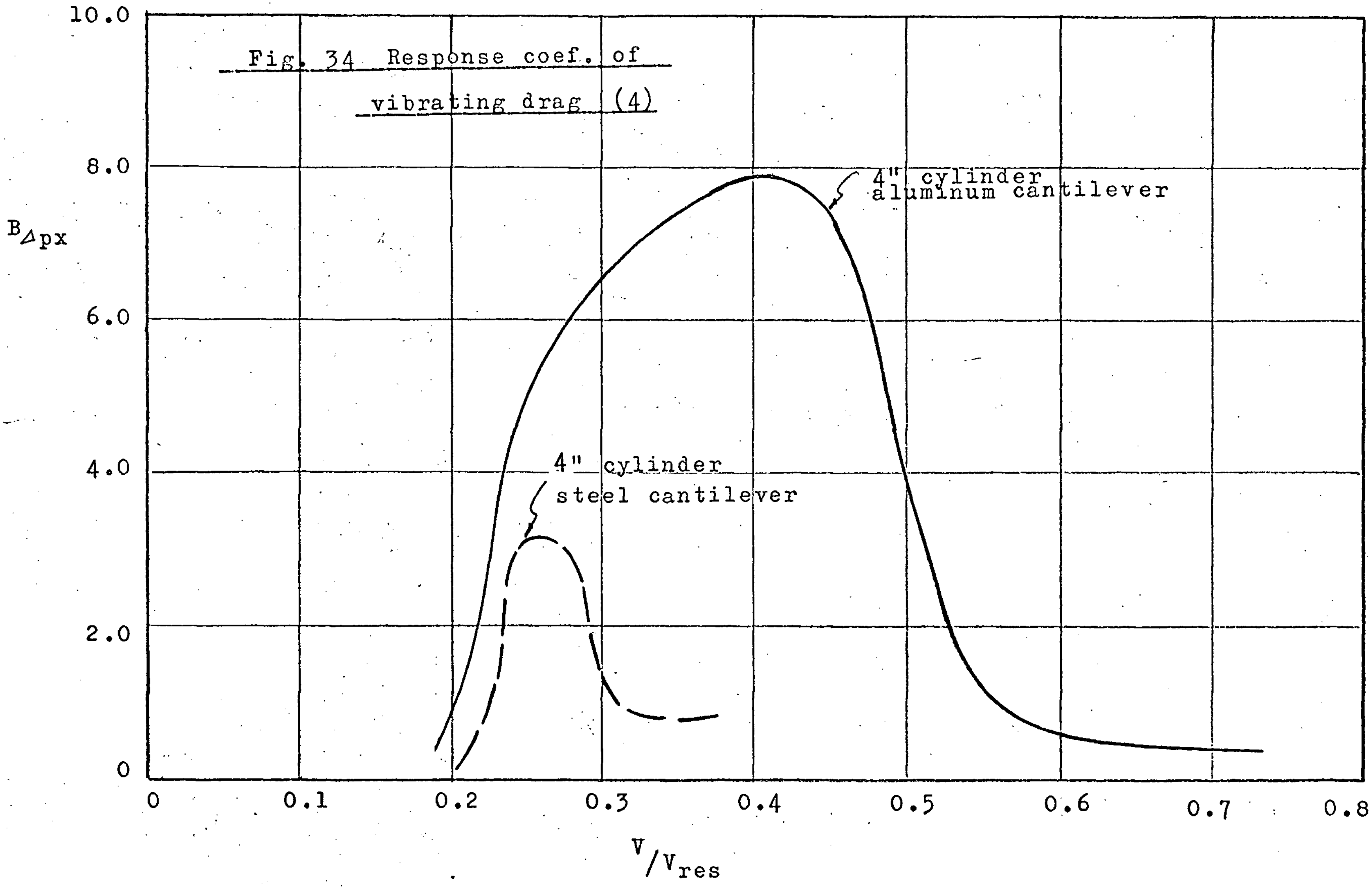

Fig. 34 Response coef. of vibrating drag (4)

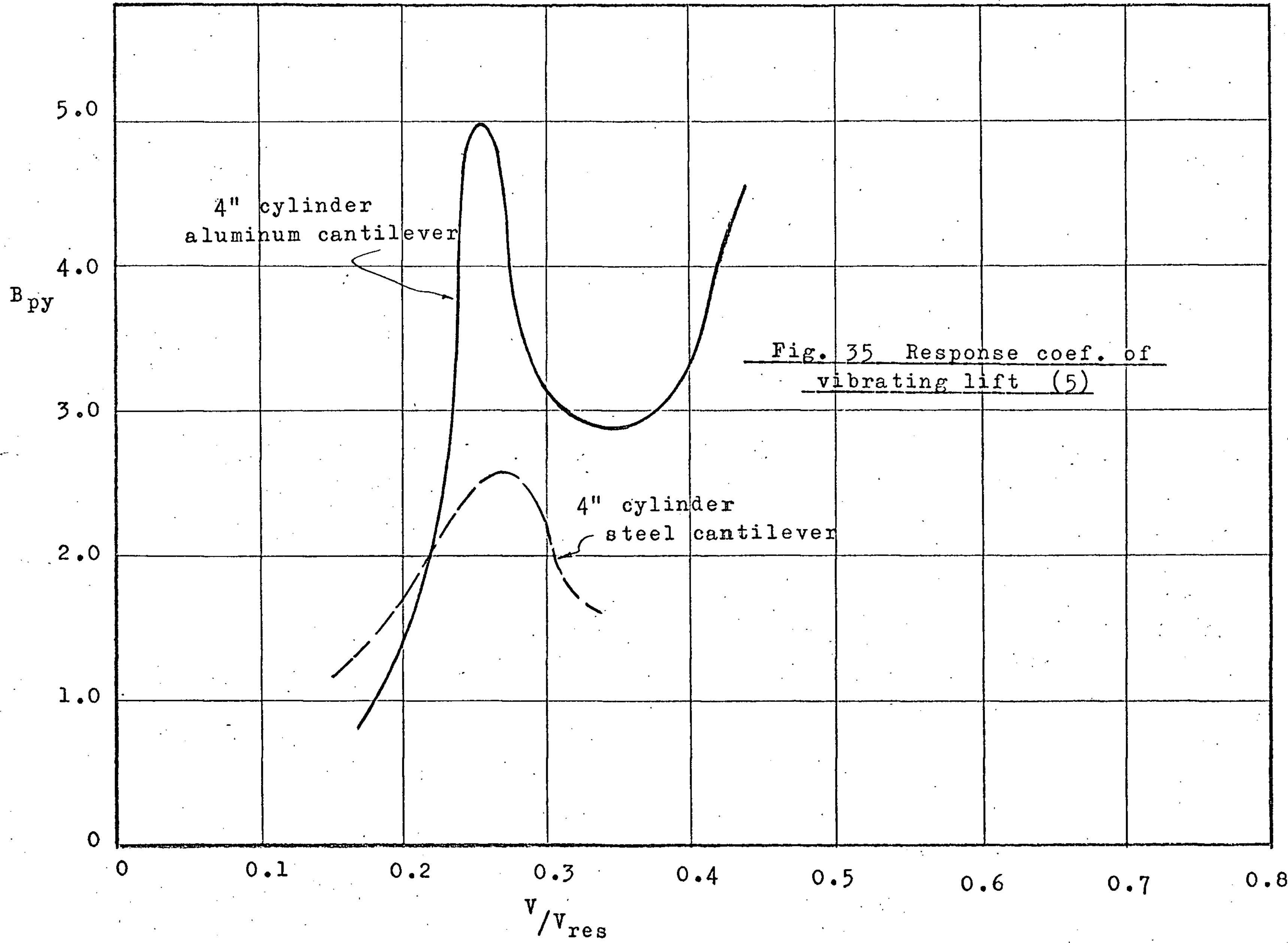

Fig. 35 Response coef. of vibrating lift (5)

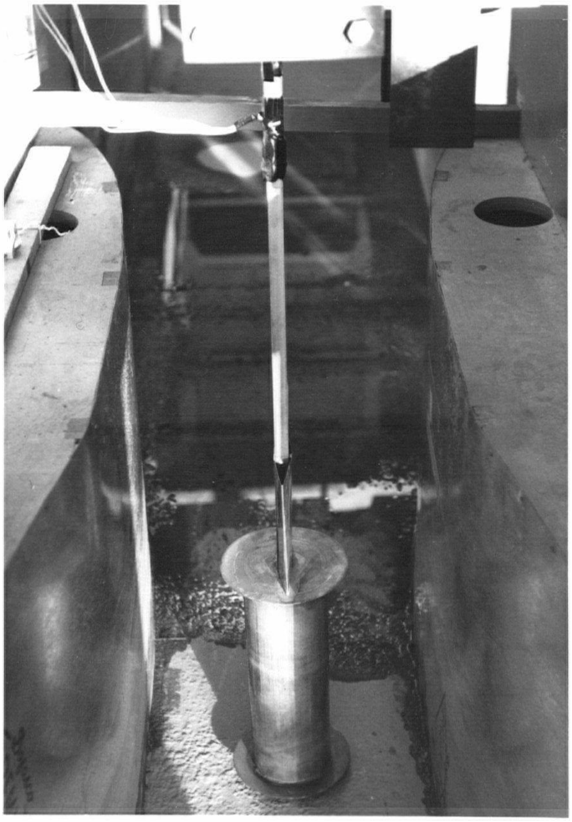

Fig. 36 Water flume and test body

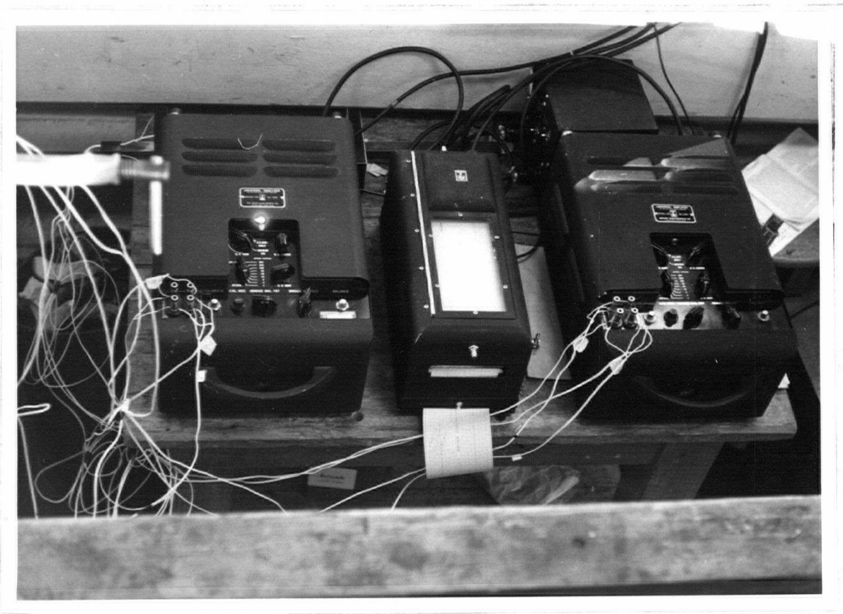

Fig. 37 Oscillograph and marking pen

Fig. 38 Cylinder vibrating near longitudinal resonance

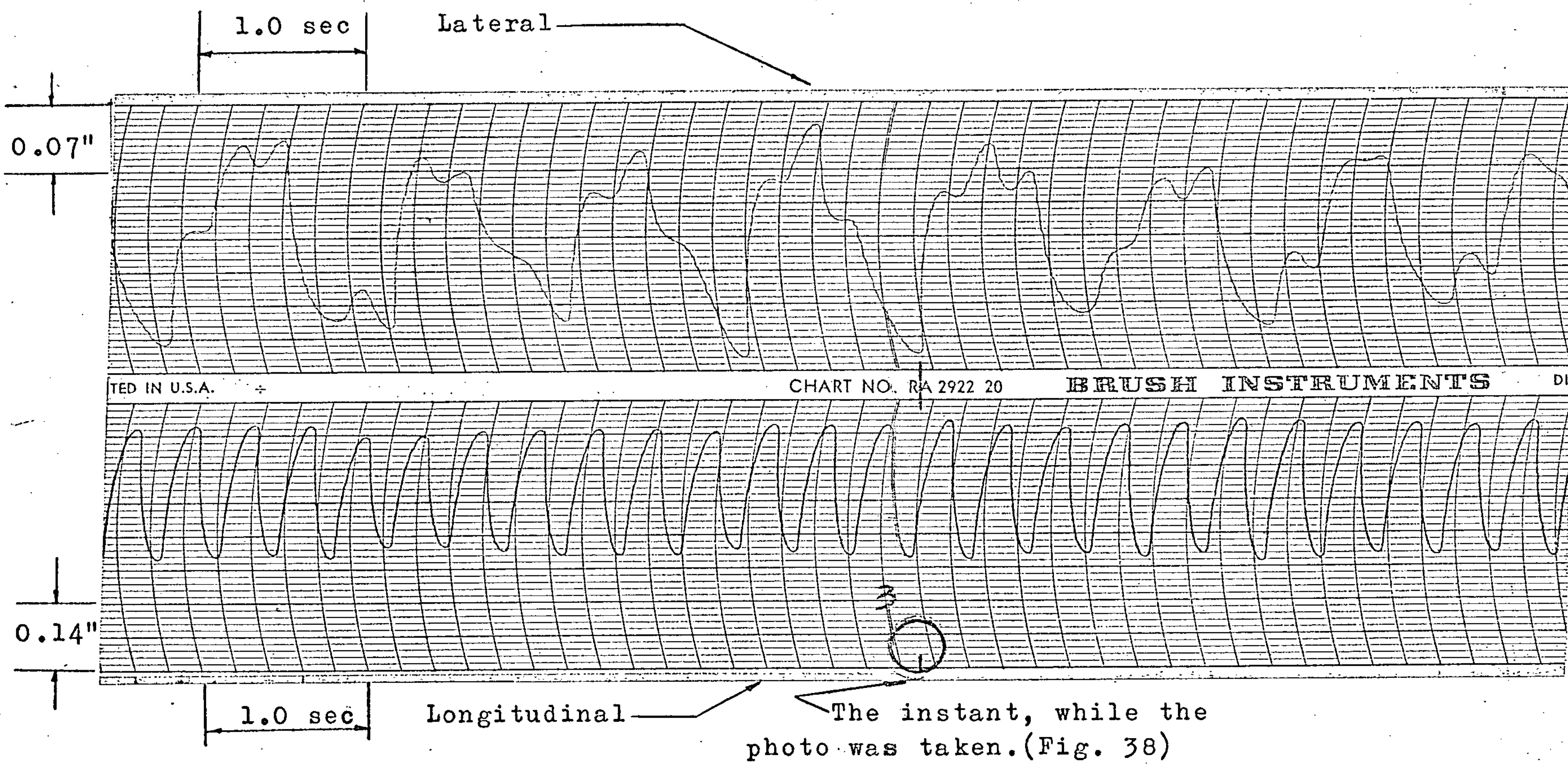

$U = 1.44$ fps
$f_x = 14.5$ cps
$f_y = 4.6$ cps

4" cylinder
aluminum cantilever
Camera speed: 1/25 sec
with white floats on surface of water

Fig. 39 Two-dimensional vibration